Geothermal history and petroleum generation in the Norwegian South Viking Graben revealed by pseudo-3D basin modelling

H. Justwan[a*], I. Meisingset[b], B. Dahl[a], G.H. Isaksen[c]

[a] Department of Earth Science, University of Bergen, Allegaten 41, 5007 Bergen, Norway.
[b] Aker Kvaerner Geo AS, PO Box 242, Lilleaker, 0216 Oslo, Norway.
[c] ExxonMobil Exploration Company, 233 Benmar, Houston, Texas 77210, USA.

Abstract

Hydrocarbon exploration in the Norwegian South Viking Graben (57º45' N to 60º15' N) began in the late 1960's and has now entered a mature phase. A map-based pseudo-3D basin modelling study is performed in order to unravel regional trends in hydrocarbon generation and expulsion and to evaluate the remaining potential of this mature petroleum province. Generation and expulsion from all major source rock horizons in the area, the Draupne, Heather, Hugin and Sleipner formations, is simulated using a pseudo-3D model comprising 36 isochronous geological events. The map based pseudo-3D model is built from 1D models combined with subsurface and source rock quality maps.

Hydrocarbon expulsion from the Middle and Upper Jurassic source rocks in the area occurred in two major phases. The first phase lasted from Paleocene to Middle Miocene with peak oil and gas expulsion during the Lower Miocene. The second, Quaternary phase of expulsion, which supplies 11 % and 13 % of all oil and gas, respectively, is related to increased subsidence rates during this period. A total of 74198 x 10^6 Sm^3 oil and 8218 x 10^9 Sm^3 gas has been expelled in the area. The Frigg Area in the north is with 2.9 x 10^{12} Sm^3 gas expelled the most gas-prone area, and the Greater Balder Area seems to be the most oil-prone area with 17 x 10^9 Sm^3 oil expelled. The lower, syn-rift section of the Upper Jurassic Draupne Formation dominates oil expulsion (54 % of all expelled oil), whilst the Heather Formation dominates gas expulsion with 38 % of all gas expelled.

Model predictions were successfully applied to explain the fill and secondary alteration history of the Greater Balder Area, Norway. The modelling supports the Draupne Formation origin of the oils in the Greater Balder Area as well as the presence of oils deriving from multiple charge phases found in correlation studies.

Based on the modelled cumulative volumes expelled and estimates for in-place volumes in the area, generation-accumulation efficiencies of 1.01-1.06 % for oil and 9.67-12.89 % for gas have been estimated for the South Viking Graben. In light of comparisons with other petroleum systems and critical evaluation of the elements of the petroleum systems, the estimated generation-accumulation efficiencies should be regarded as encouraging for further exploration of the area.

Keywords: *North Sea; South Viking Graben; Basin Modelling, Petroleum Systems*

*   Corresponding author. Tel.: +47 55588116; Fax: +47 55583660
       E-mail address: holger.justwan@geo.uib.no (H. Justwan).

1. Introduction

Over 323 x 10^6 Sm^3 of oil and 464 x 10^9 Sm^3 of gas (recoverable) have been discovered in the petroleum systems of the Norwegian South Viking Graben (Ministry of Petroleum and Energy, 2005). The majority has been discovered in clastic reservoirs of Paleocene and Eocene age. Upper and Middle Jurassic as well as Triassic sandstones have also been found to be hydrocarbon bearing. Principal source rocks are the Upper Jurassic Heather and Draupne formations (Field, 1985; Isaksen and Ledje, 2001; Justwan et al., 2005) and to a lesser extent the Middle Jurassic Hugin and Sleipner Formation (Isaksen et al., 2002; Justwan et al., 2006). After nearly 40 years of exploration and drilling of 270 exploration wells as well as 279 development wells in the Norwegian sector of the South Viking Graben, the size and frequency of discoveries appears to decline. The area is now regarded to have reached a mature phase of exploration (Østvedt et al., 2005).

This paper is the third part of an integrated study of the petroleum systems of this mature exploration area. This integrated study includes source rock analysis and mapping (Justwan and Dahl, 2005; Justwan et al., 2005) as well as oil-source correlation (Justwan et al., 2006). This paper discusses the geohistory of the Norwegian South Viking Graben between 57º45' N to 60º15' N and presents a quantitative estimation of the oil and gas expelled. Previously published basin modelling studies in the region only focussed on smaller subareas, such as the Sleipner area (Wei et al., 1990), or covered the South Viking Graben as part of a larger geographical area at a reduced level of detail (e.g.
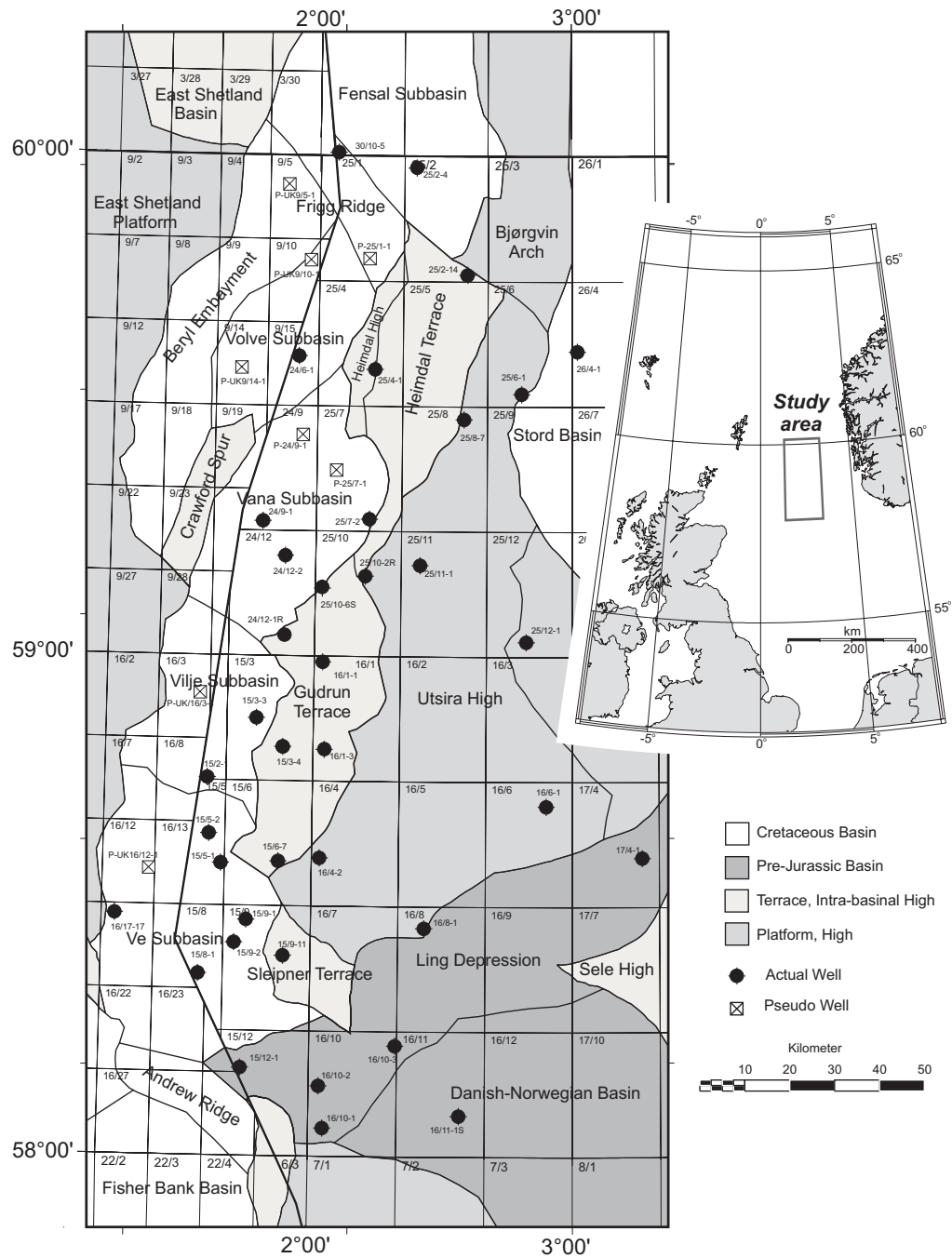
Fig. 1. Overview map of the study area displaying 1D modelling sites and pseudo-wells used. Structural elements are taken from NPD (2005).

Baird, 1986; Kubala et al., 2003). The evaluation of the petroleum systems and the remaining potential of the area are warranted by the need for improved understanding of the hydrocarbon systems in the area since rising oil prices increased the interest in small satellite fields and smaller prospects. In view of this, the overall remaining resources in the area are evaluated through calculation of generation-accumulation efficiencies. The model will also be used to evaluate the petroleum systems of a subarea of the South Viking Graben, the Greater Balder Area.

2. Geological Setting

The present day structural configuration and stratigraphy of the area from 57° 45' to 60° 15' N (Fig. 1) are the result of two major phases of extension. They are followed by a long period of thermal subsidence accompanied by several phases of compressional tectonics and uplift.

The first period of rifting occurred at the transition of the Permian and Triassic (Ziegler, 1990) with extension affecting the entire area (Færseth, 1996) and estimated stretching factors between 1.28 and 1.41 (Odinsen et al., 2000). The Permo-Triassic rifting event was followed by a period of post-rift cooling in early to Middle Jurassic times (Steel and Ryseth, 1990; Coward et al., 2003). Uplift at the triple junction of Central, Viking and Witch Ground Graben from late Toarcian to Callovian caused significant erosion of underlying sequences (Underhill and Partington, 1993) and supplied erosional products to be redeposited in deltaic complexes, such as the Brent delta (Graue et al., 1987). The second phase of extension in the area followed in Bajocian to Volgian times (Rattey and Hayward, 1993; Fraser et al., 2003) and appears to be smaller in overall magnitude than the previous phase (Odinsen et al., 2000). Extension during this second phase was more localised and affected mainly the Viking Graben with β factors of 1.42 to 1.53 (Odinsen et al., 2000) in the west, while the Stord Basin in the east remained largely unaffected (Færseth, 1996). After cessation of the rifting in the Middle Volgian (Rattey and Hayward, 1993; Fraser et al., 2003), passive thermal subsidence prevailed throughout the Cretaceous, and uplifted footwall highs were gradually onlapped and covered (Coward et al., 2003). Uplift related to the development of the Iceland plume in the earliest Tertiary (Nadin and Kusznir, 1995) caused significant erosion and supplied large quantities of clastic sediments (Jenssen et al., 1993; Jordt et al., 1995). After decay of the uplift in the Eocene, three significant phases of post-Eocene uplift of the Shetland Platform, the northern North Sea basin and southern Fennoscandia resulted in erosion and subsequent deposition of sand-rich sediments in the Oligocene and Miocene (Rundberg and Eidvin, 2005). The Pleistocene is governed by glacially induced subsidence, isostatic adjustments (Riis and Fjeldskaar, 1992; Jordt et al., 1995) and a sharp acceleration in sedimentation rates (Ziegler, 1990).

3. Model building

3.1. Strategy

The burial history and thermal evolution of the area has been investigated by means of one dimensional basin modelling and subsequent generation of a pseudo-3D model (Fig. 2). The geohistories, comprising 36 isochronous layers, of 38 wells (Fig. 1 for well locations) have been simulated for this purpose using a forward modelling approach with the basin modelling software *TERRAMOD*®. Optimisation of the individual 1D models was achieved by calculation of vitrinite reflectance using a modified TTI approach and comparison with measured data. Corrected borehole temperatures from wireline logs and DST temperatures as well as hopane and sterane isomerisation, calculated using a first-order kinetic model, were used as check parameters. Four component (C_{15+}: heavy oil, C_{6-14}: light oil, wet gas: C_{2-5} and dry gas: C_1) compositional kinetic schemes were used for thermal modelling. The principal model output from all the modelled wells including vitrinite reflectance, transformation ratios for the four modelled pseudo-components, temperature, subsidence history and calculated porosities was then transferred via the *BASXYZ* interface to the *BasinAssist* module of the mapping software package *IRAP*® (Dahl and Meisingset, 1996). A map based pseudo-3D model has been created in *IRAP*® from 1D simulation results, subsurface and paleo-water depth maps as well as source rock quality and thickness data (Fig. 2). At this point pseudo-wells can be easily created in the model, and the data can be fed back into the 1D modelling loop (Fig. 2). In total, 8 pseudo-wells have been created (Fig. 1), and their geohistory has been modelled to improve the data coverage in the undrilled portions of the graben centre. The next step involves mapping of transformation ratios for four pseudo-components using a kriging approach with external drift. Incremental generated and expelled hydrocarbon volumes are calculated based on maps of the transformation ratio for various timesteps and source rock potential maps. The general workflow (Fig. 2) of this map-based system has been described in Dahl and Meisingset (1996).
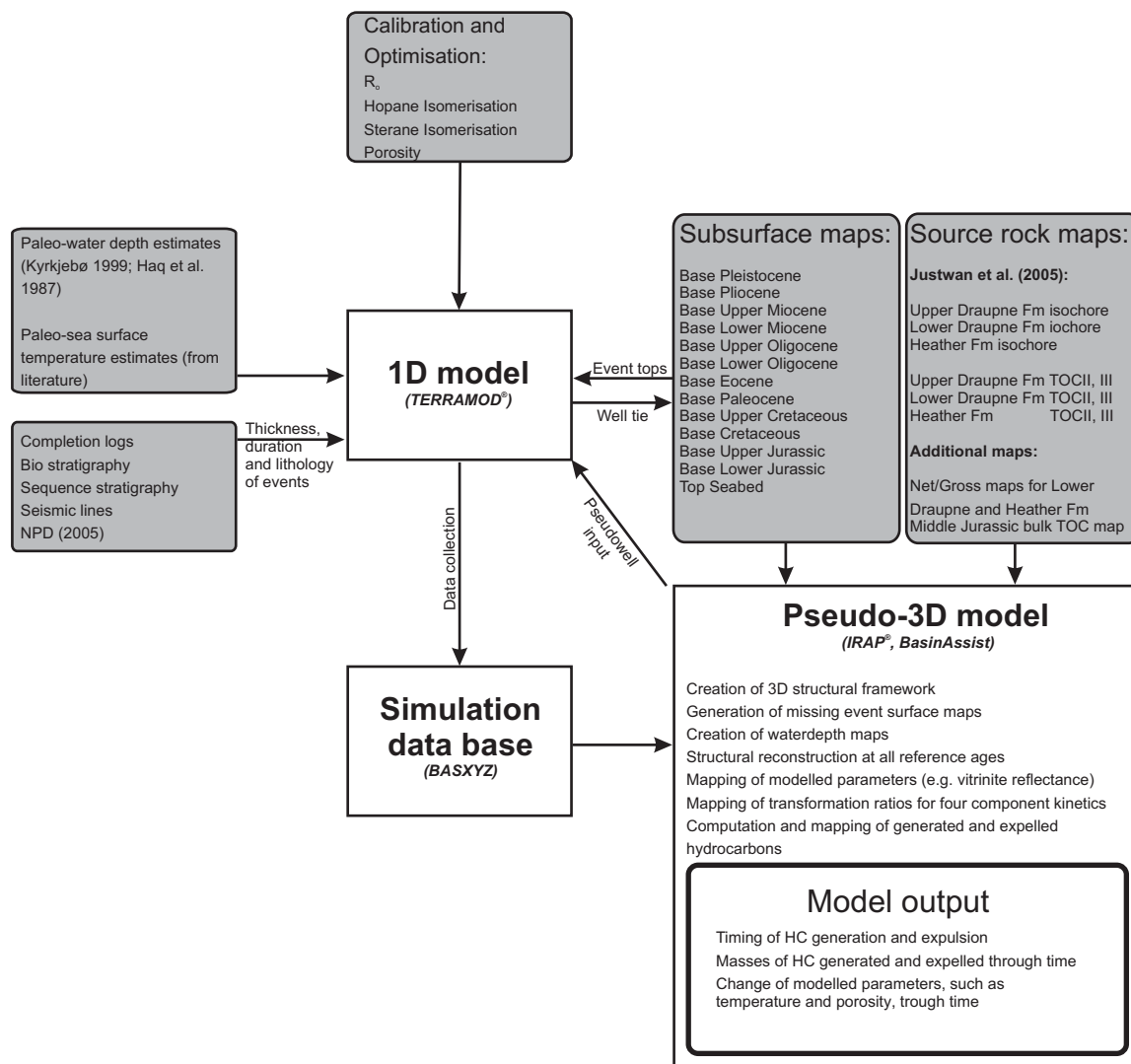
Fig. 2. Chart illustrating the work flow and input data for this pseudo-3D basin modelling study. Input data is shown by shaded boxes, while essential model parts are shown by white boxes.

3.2. 1D conceptual model

3.2.1. Model input

Input for the individual 1D models are thicknesses, duration and type (depositional, non-depositional and erosional) of the 36 isochronous modelling events. In addition, lithologies, paleo-water depths, paleo-temperatures, porosities, heatflow estimates as well as hydrocarbon generation kinetics are required. The duration of the respective units is based on published dates, completion logs and Esso's proprietary sequence stratigraphic framework. The age scale of Berggren et al. (1995) for the Cenozoic and Hardenbol et al. (1998) for the Mesozoic has been applied. Paleo-bathymetry is critical for paleo-subsurface topography and resulting structural configuration, which affects burial and maturation of the source rocks as well as secondary migration pathways. Therefore, it has to be evaluated for critical time periods. The paleo-water depths used in this study are based on the work of Kyrkjebø (1999), who used an integrated approach using both micropaleontological data and tectonic modelling to create maps for 12 timesteps (Fig. 3). Water depths for the remaining events have been interpolated from these values using the global sea-level curve of Haq et al. (1987). Paleo-temperatures are another important input parameter because they both affect heatflow as well as the temperature history directly. Our estimates are based on published sea surface temperatures (e.g. Buchardt, 1978; Levitus and Boyer, 1994; Zachos et al., 2001; Poulsen and Riding, 2003; Jenkyns et al., 2004). They have been corrected for water depths using a global reduction of 2.5° C for the first 100 m followed by further 2° C for every 100

m of the remaining water depth to a minimum of 2º C based on average present day gradients from Levitus and Boyer (1994). Event lithologies have been chosen from 70 predefined lithologies to match information from completion logs and rock sample descriptions. Total matrix porosities have been determined by iterative model optimisation and thickness matching. Measured porosities were used as a check parameter, where available. Heatflow histories have been determined by model optimisation and will be discussed below. Generation from Upper Jurassic source rocks was modelled using hydrocarbon generation kinetics after Burnham and Dahl (1993), while the kinetic scheme of Espitalié et al. (1988) was used for Middle Jurassic sources.

3.2.2. Model event subdivision

Subdivision of the stratigraphic column into isochronous geological events is the most critical model input. The sedimentary section in the South Viking Graben has been subdivided into 29 depositional and 7 non-depositional events of Lower Jurassic to Quaternary age (Fig. 3) based on the sequence stratigraphic framework of Esso and well completion logs. This is complemented by information from seismic lines, subsurface maps and NPD (2005) (Fig. 2). The resulting subdivision has been harmonised with available subsurface maps provided by Esso Norway. Thicknesses for Upper Jurassic units are taken from Justwan et al. (2005).

3.2.2.1. Jurassic event subdivision

The Jurassic section has been subdivided into eight model events beginning with the sandstones and mudrocks of the Statfjord Formation of Rhaetian to Aalenian age (Fig. 3). The Statfjord Formation is overlain by the marine clastics of the Lower Jurassic Dunlin Group, which comprises two events. Regional uplift and doming at the triple junction of Viking-, Central and Witch Ground Graben began in the late Toarcian and led to a systematic truncation of Lower Jurassic strata (Partington et al., 1993). Dunlin sediments can therefore generally only be found north of 59º in the studied wells, and Upper Dunlin sediments (event 3) have only been encountered in Well 26/4-1 (location see Fig. 1). The section of Aalenian to Bajocian age which corresponds to the topmost Dunlin Group and lowermost Brent Group is absent throughout the study area and is therefore modelled as a hiatus (Fig. 3). In principle, the truncation of Lower Jurassic strata should have been modelled as an erosional event. The exact magnitude can, however, not be determined and is irrelevant for the maturation of the younger, overlying Middle and Upper Jurassic source rocks. The Lower Jurassic Dunlin shales have been inferred as the source for the gas of the Frigg Field (Jones et al., 2003). They are, however, reported to be lean and inertinitic in the study area, and their actual contribution to the generated hydrocarbons is disputed (Thomas et al., 1985; Husmo et al., 2003). As a consequence, they have not been considered as a source event in this study.

The regional uplift supplied large volumes of sediment and led to the deposition of the Brent delta beginning in the Aalenian (Graue et al., 1987) (event 5). After its initial advance, a Bajocian-Bathonian eustatic sea-level rise, along with reduced sediment supply, led to the retreat of the delta and the formation of stacked marine sandsheets (Tarbert and Hugin Formations), which interfinger landwards with a deltaplain succession (Upper Ness and Sleipner Formations) (event 5) (Graue et al., 1987). The shales, carbargillites and coals within event 5 are considered to be source for gas and minor amounts of volatile oil in the area (Larsen and Jaarvik, 1981; Isaksen et al., 2002; Justwan et al., 2006). Event 5 has therefore been modelled as a source rock event.

The main source rock units in the area, the shales and sands of the Heather (event 6) and the shales of the Draupne Formation, have been deposited during subsequent sea-level rise (e.g. Field, 1985; Isaksen and Ledje, 2001; Justwan et al., 2005). The Draupne Formation can be subdivided into a lower, syn-rift section of Oxfordian to Middle Volgian age (event 7) and a post-rift section of Middle Volgian to late Ryazanian age (event 8) (Rattey and Hayward, 1993). These sections show large differences in source facies and hydrocarbon potential (Isaksen and Ledje, 2001; Justwan and Dahl, 2005; Justwan et al., 2005). The Middle and Upper Jurassic events are not strictly isochronous, although they are regarded as such in the model (Fig. 3). Perturbation analysis on a shallow and a deep well was performed to assess the effect of the inaccuracy in age on the model output but has shown no significant changes.

Fig. 3. Generalised litho- and chronostratigraphic framework of the South Viking Graben including subdivision in 36 isochronous model events. Cenozoic ages are based on the timescale of Berggren et al. (1995), while Mesozoic ages are based on the scale in Hardenbol et al. (1998). Lithostratigraphic nomenclature follows Vollset and Doré (1984) and Isaksen and Tonstad (1989). The global sea-level curve is taken from Haq et al. (1987) and the paleo-temperature curve shows sea-surface temperature model input and is based on the literature (see text). The remarks column contains information on available subsurface maps (Map horizon), water depth maps from Kyrkjebø (1999) (Water depth) and relates some of the surfaces to the CSS surfaces of Jordt et al. (1995).

Event 9 (Fig. 3) represents the most prominent unconformity in the area: the near base Cretaceous unconformity. This event is polychronous (Kyrkjebø, 1999) and often a complex amalgamation of several unconformities or a conformable boundary with a condensed section (Rawson and Riley, 1982; Rattey and Hayward, 1993). According to Rattey and Hayward (1993), it represents the final failure of the North Sea rift with transfer of extension to the Atlantic margin. Event 9 can be best described for modelling purposes as a period of non-deposition of approximately 10 Ma duration.

3.2.2.2. Cretaceous event subdivision

The Lower Cretaceous is characterised by a major basin wide change from deposition of anoxic shales in the Upper Jurassic to carbonates and calcareous shales (Rawson and Riley, 1982; Copestake et al., 2003) during a general sea-level rise (Haq et al., 1987). The Lower Cretaceous has been subdivided into four events (Fig. 3) beginning with the Barremian to Hauterivian calcareous claystones of the Åsgard Formation (event 10). This event is followed by a stratigraphic break (event 11) related to the Austrian tectonic event (Ziegler, 1990). The Sola Formation, consisting of shales with interbedded marlstones and limestones, forms event 12 and is overlain by the late to mid Albian Rødby Formation (event 13). The top of the Rødby Formation marks the top of the Lower Cretaceous, where a global highstand in sea-level reduced clastic input (Ziegler, 1990; Oakman and Partington, 1998) and gave way to Chalk deposition in the Upper Cretaceous.

The Upper Cretaceous in the study area was subdivided into four events (Fig. 3) based on Isaksen and Tonstad (1989), Hardenbol et al. (1998), Oakman and Partington (1998), Surlyk et al. (2003) and the sequence stratigraphic framework of Esso. Subdivision is complicated by a very prominent facies change from the south to the north of the study area. The carbonate dominated Chalk Group interfingers between 58°30' and 60° with the siliciclastic Shetland Group. The Cenomanian chalky limestones of the Svarte Formation and its mudstone-dominated time equivalent, the Hidra Formation, constitute event 14. The basal section of the overlying event 15, the Black Band within the Blodøks Formation, is a basin-wide correlative event of stagnant, partly anoxic conditions (Surlyk et al., 2003). Event 15 comprises the latest Cenomanian to Middle Turonian Blodøks and Tryggvason formations and equivalent sections of the limestones of the Hod Formation (Fig. 3). The siliciclastic Kyrre Formation and lowermost Jorsalfare Formation as well as the carbonate-prone upper Hod Formation form event 16. Event 17 includes the chalks of the Tor Formation and the time equivalent siliciclastic section of the Jorsalfare Formation. The top of the Tor Formation is developed as hard ground and represents a regional unconformity (event 18) at the Cretaceous-Tertiary boundary (Isaksen and Tonstad, 1989; Surlyk et al., 2003).

3.2.2.3. Tertiary event subdivision

Clastic input increases at the top of the Maastrichtian, and chalk deposition temporarily stops until it resumes for a short period in the Danian Ekofisk Formation (event 19) (Neal, 1996; Oakman and Partington, 1998). The calcareous section of the overlying Maureen, Ty and Våle Formations was regarded to be of Danian age (event 19) when dating was not available, while the siliciclastic section was assigned to the overlying event 20. After retreat of the Chalk seas, regional uplift of the East Shetland Platform and the Scottish Highlands, related to the development of the Iceland plume, resulted in erosion and redeposition of material as deep marine sandstones in events 20 to 22 (Isaksen and Tonstad, 1989; Jenssen et al., 1993; Bergslien, 2002).

Submarine fan sandstones of the Heimdal Formation, which are very important reservoir units in the area, and interbedded hemipelagic muds of the Lista Formation, equalling zones IB and IA2 of Jenssen et al. (1993), form event 20. Event 21 also includes important reservoir intervals in the submarine fan sandstones of the Hermod Formation, which are surrounded by hemipelagic mud of the Sele Formation and equal zone II of Jenssen et al. (1993). Igneous activity in the North Atlantic province and relative rise in sea-level are responsible for the tuffaceous sediments of the Balder Formation (event 22) (Jordt et al., 1995). This isochronous event is a seismic marker horizon and usually associated with the Base of the Eocene. Event 22 is followed by a minor hiatus at the top of the Balder Formation (Neal, 1996; Martinsen et al., 1999).

Eocene strata have been divided into two units (Fig. 3) in this study following Mudge and Bujak (1994). The lower Frigg sequence (event 24) of Ypresian to Lutetian age contains the basinal mudstones of the Horda Formation and the sandy Frigg Formation. Event 25 equals the Alba and Grid sequences of Mudge and Bujak (1994) and includes the blocky sands of the Grid Formation.

Influence of the Pyrenean orogeny resulted in a widespread unconformity seen on top of the Eocene (event 26) (Gradstein and Backstrom, 1996; Martinsen et al., 1999; Rundberg and Eidvin, 2005). The monotonous mudstone deposition in the Oligocene complicates the subdivision of the Oligocene section (Neal, 1996). A marked sea-level fall occurred in the mid Oligocene (Jordt et al., 1995; Martinsen et al., 1999), and its seismic and log expression was used by Jordt et al. (1995) to subdivide the Oligocene. This subdivision has been adopted for this study, and dating from completion logs, gamma ray log correlation and available subsurface maps were used for subdivision.
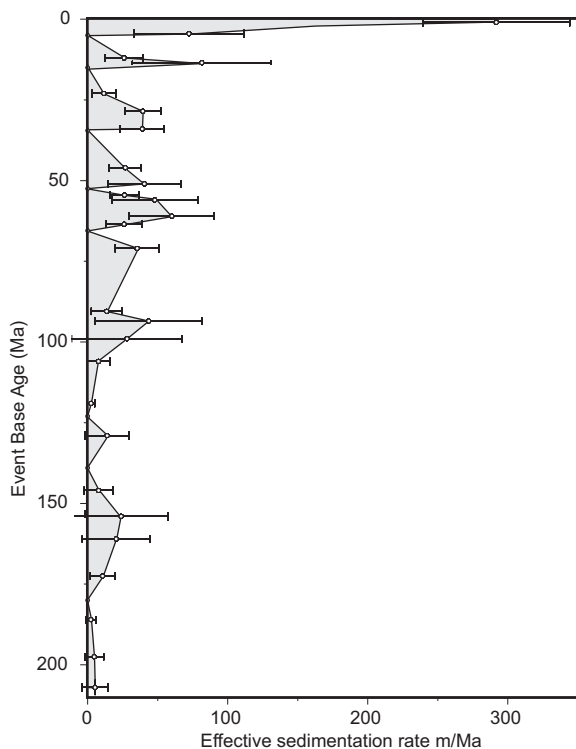

Fig. 4. Average sediment accumulation rates for the model events of all modelled well sites. While accumulation rates are well below 100 m/Ma for events 1 to 34, Quaternary accumulation rates exceed 300 m/Ma. Bars indicate the standard deviations.

Miocene sediments conformably overlie Oligocene strata in the South Viking Graben (Rundberg and Eidvin, 2005). In the early Miocene, the turbiditic sands of the Skade Formation and associated hemipelagic sands have been deposited (event 29). Progressive uplift of the northern North Sea basin occurred in the Oligocene to Miocene and resulted in a shallowing of the basin (Rundberg and Eidvin, 2005). A distinct mid to late Miocene compressional phase is responsible for the development of a mid Miocene unconformity (Løseth and Henriksen, 2005). This event (30) is very prominent in the northernmost North Sea, where it spans 20 Ma and includes severe erosion (Løseth and Henriksen, 2005; Rundberg and Eidvin, 2005). It spans only ca. 1.5 Ma in the study area (Rundberg and Eidvin, 2005), where no major erosion is evident (Y. Rundberg, pers. comm.). Event 31 represents a basin filling sequence onlapping the Lower Miocene and consists mainly of mudstones with thin sandy intervals (Rundberg and Eidvin, 2005). Event 32 comprises the sandy Utsira Formation.

Subdivision of the Miocene is difficult due to poor seismic resolution, problems with biostratigraphic dating as well as inconsistencies in the lithostratigraphic definition of units (Rundberg and Eidvin, 2005). Therefore, older subdivisions on well logs have been disregarded, and the revised lithostratigraphic and chronostratigraphic subdivision of Rundberg and Eidvin (2005) has been used (Fig. 3). Miocene units are followed by a Base Pliocene hiatus (event 33) of short duration (Martinsen et al., 1999), which has been related to starved sedimentation caused by relative sea-level rise (Gregersen et al., 1997). Pliocene sediments in the area (event 34) were deposited in a simple westward prograding wedge as a result of uplift of the Scotland Shetland area (Jordt et al., 1995; Martinsen et al., 1999). The uplift culminated in the tilting of the Stord Basin in the east of the study area and the adjacent basin margin and resulted in a prominent angular unconformity in this region (Ghazi, 1992).

3.2.2.4. Quaternary event subdivision

To the east of the study area and in the Norwegian Channel, Pleistocene erosional truncation is evident (Sejrup et al., 1995), but Cameron et al. (1987) observed that the transition may be conformable in the deeper parts of the basin. The contact between Quaternary and Pliocene units was therefore considered to be conformable in this area. The

Quaternary section is subdivided based on lithology and interpretation of seismic data into two events (35 and 36) (Fig. 3). They correspond largely to the CSS9 and CSS10 sequences of Jordt et al. (1995). The Quaternary shows sharp acceleration of subsidence rates and deposition in marine to glaciomarine environment. A comparison of average sediment accumulation rates for all modelled sites reveals clearly the increased magnitude of Quaternary sedimentation with average rates reaching up to 300 m/Ma, as opposed to about 50 m/Ma for older events (Fig. 4). A number of minor stratigraphic breaks have been recorded in the Pliocene and above (Martinsen et al., 1999). Their duration, however, is too short to be of relevance for the modelling.

3.2.3. Source rock events and properties

The Hugin and Sleipner Formation of event 5 and the Draupne and Heather Formation including events 6, 7 and 8 constitute the main source rocks in the area (Field, 1985; Isaksen and Ledje, 2001; Isaksen et al., 2002; Justwan et al., 2005).

The shales, carbargillites and coals of the Middle Jurassic (event 5) in the South Viking Graben span a wide range of TOC and HI values (Justwan et al., 2005) and are best described as containing coaly Type III kerogen. Maturity corrected TOC and HI values range from 0.2 to 47.8 wt% and 41 to 641 kg HC/t C_{org} (n=150) for shales and from 52.7 to 91.7 wt% and 178 to 368 kg HC/t C_{org} for coals (n=15). Due to the heterogeneity of the Middle Jurassic, the oil and gas potential of this section has not been evaluated in this study. Rock-Eval data, however, appear to confirm the conclusion of Isaksen et al. (2002) that the Middle Jurassic source rocks are mainly gas-prone with only minor oil potential. Field (1985) indicates coal thicknesses of more than 30 m in the axial parts of the graben, whereas well log analysis of the 38 modelled 1D sites showed a maximum thickness of up to 56 m in Well 25/7-2.

The Heather Formation (event 6) in the study area is lean and mostly gas-prone with average maturity-corrected hydrogen indices of 184 g HC/kg C_{org} and average TOC values of 3.6 wt% and reaches thicknesses of 930 m (Justwan et al., 2005; 2006). The Draupne Formation can be subdivided into a syn-rift section, up to 1600 m thick (event 7, "lower Draupne"), and a thinner (330 m) post-rift section (event 8, "upper Draupne") (Justwan et al., 2005). The syn-rift section shows large quality and facies variation caused by varying degrees of oxygenation and dilution processes. The content of gas-prone material is high in the syn-rift section with average maturity corrected TOC values of 4.1 wt% and HI of 234 g HC/kg C_{org}. The post-rift section, on the other hand, represents a highly oil-prone shale blanket deposited after cessation of the rifting activity in the Upper Jurassic (Justwan et al., 2005). Average maturity corrected TOC and HI values amount to 5.3 wt% and 340 g HC/kg C_{org} in this section.

3.2.4. 1D model optimisation and heatflow history

The heatflow history is an important input to the 1D models but is often difficult to constrain. Heatflow is not a directly measured parameter but a result of the geothermal gradient. The only known parameter in a heatflow history is the present day temperature. The remaining thermal history has to be determined by model adjustment and iterative comparison of observed and modelled data such as vitrinite reflectance, sterane and hopane isomerisation and bore hole temperatures. An alternative or complimentary method is the determination of heatflow as a function of subsidence using thermo-mechanical models (e.g. McKenzie, 1978).

Perturbation analysis shows that the modelled present day vitrinite reflectance, temperature and sterane and hopane isomerisation are not sensitive to heatflow input changes in the Lower Cretaceous and Jurassic, probably due to the overprint by rapid burial in the Tertiary. The heatflow histories of events 1 to 7 (207-146 Ma) are therefore conceptual and based on a geological model of the area. Heatflow increases from background values with the onset of uplift and thermal doming at the triple junction of the Viking-, Central- and Witch Ground Graben in the late Toarcian (event 4) to reach peak heatflow values during the most intense phase of Jurassic rifting in the Volgian (event 7) (Fig. 5a). Thermo-mechanical modelling to constrain peak heatflow values in the Jurassic has not been performed, but the peak heatflow values are based on published data from the nearby North Viking Graben in Dahl and Yükler (1991) (Fig. 5b) and Dahl and Augustson (1993). Peak heatflow values were assigned to different parts of the study area based on the principle that heatflow generally decreases away from the heat source in the axial graben portions. The area was therefore subdivided into three provinces including graben, flank and high, with peak heatflow
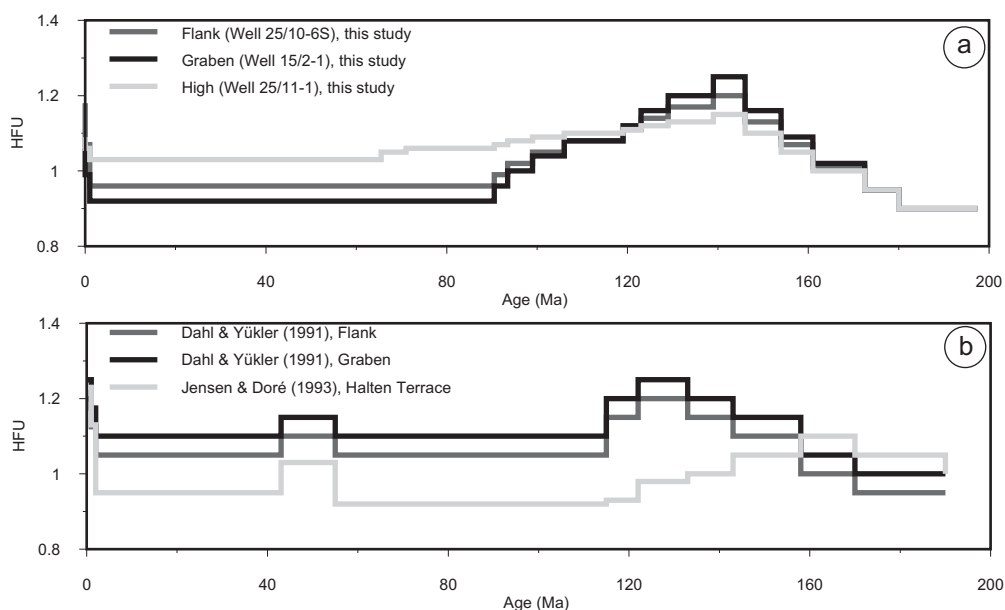
Fig. 5. (a) Heatflow input concept illustrated for three well locations in the study area (locations see Fig. 1). While the Jurassic heatflow input is conceptual, Cenozoic heatflow is the result of model iterations to match observed data. In order to match present day observed temperatures, a Quaternary heatflow increase is necessary. (b) Similar heatflow scenarios have been used by Dahl and Yükler (1991) for the North Viking Graben and Jensen and Doré (1993) for the Halten Terrace. For well locations see Fig. 1.

values of 1.25, 1.2 and 1.15 respectively (Fig. 5a). Differences in maximum heatflow during events 1 to 7 have probably little effect on hydrocarbon generation since the source rocks at that time are barely buried. The rate of heatflow decay after cessation of rifting activity is a qualitative estimate for every 1D simulation and is based on the subsidence history. Periods of fast subsidence generally correspond to fast heatflow decrease.

Various heatflow scenarios have been tested for the Tertiary. It appears that a constant Tertiary heatflow is sufficient to match observed vitrinite reflectance as well as sterane and hopane data for most of the wells. In order to match present day observed temperatures (DST and Horner corrected log temperatures), a Quaternary heatflow increase in event 35 and 36 is necessary. The heatflow values required in the Quaternary cannot be applied to the Tertiary since they result in too high vitrinite reflectances and hopane and sterane values (Fig. 6). The necessity of a Quaternary heatflow increase has been previously observed by numerous authors (e.g. Mo et al., 1989; Dahl and Yükler, 1991; Dahl and Augustson, 1993), and its significance and probable causes have been discussed by Jensen and Doré (1993). This recent heatflow increase is believed to be a transient effect. Sediments buried at depth due to loading with ice sheets during the Quaternary glaciations undergo uplift due to isostatic effects during deglaciation and have not cooled and adjusted to the present situation. A transient state and its equilibration has been modelled in the Stord Basin by Hermanrud et al. (1991)

Various authors also discuss an early Tertiary heatflow pulse related to the onset of spreading activity in the Atlantic, e.g. Dahl and Yükler (1991) and Jensen and Doré (1993). While this event might play an important role in the Norwegian Sea and the North Viking Graben, the models in the South Viking Graben are insensitive to a Tertiary heatflow pulse, most likely due to the distance of the study area to the heat source.

In order to evaluate the rigidity of the heatflow input concept, vitrinite reflectance was also calculated using the Easy%Ro algorithm of Sweeney and Burnham (1990). Easy%Ro values give also a reasonable match to observed values in the area, although all wells have been optimised using TTI-Ro (Fig. 6). On a regional scale, TTI-Ro values tend to be higher than Easy%Ro values below 4200 m depth and represent a more optimistic case for maturation, while Easy%Ro is more optimistic above 4200 m (Fig. 7). Modelling has shown that a Quaternary heating event remains necessary also when Easy%Ro is used (Fig. 6).

Mapping of the Cenozoic heatflow for all 1D sites interestingly reveals that heatflow is generally lower in the Viking Graben and tends to increase towards the Utsira High in the east. This observation is consistent with the work of Eggen (1984), Brigaud et al. (1992) and Burley (1993) proposing a heat transfer mechanism from the basin centre by
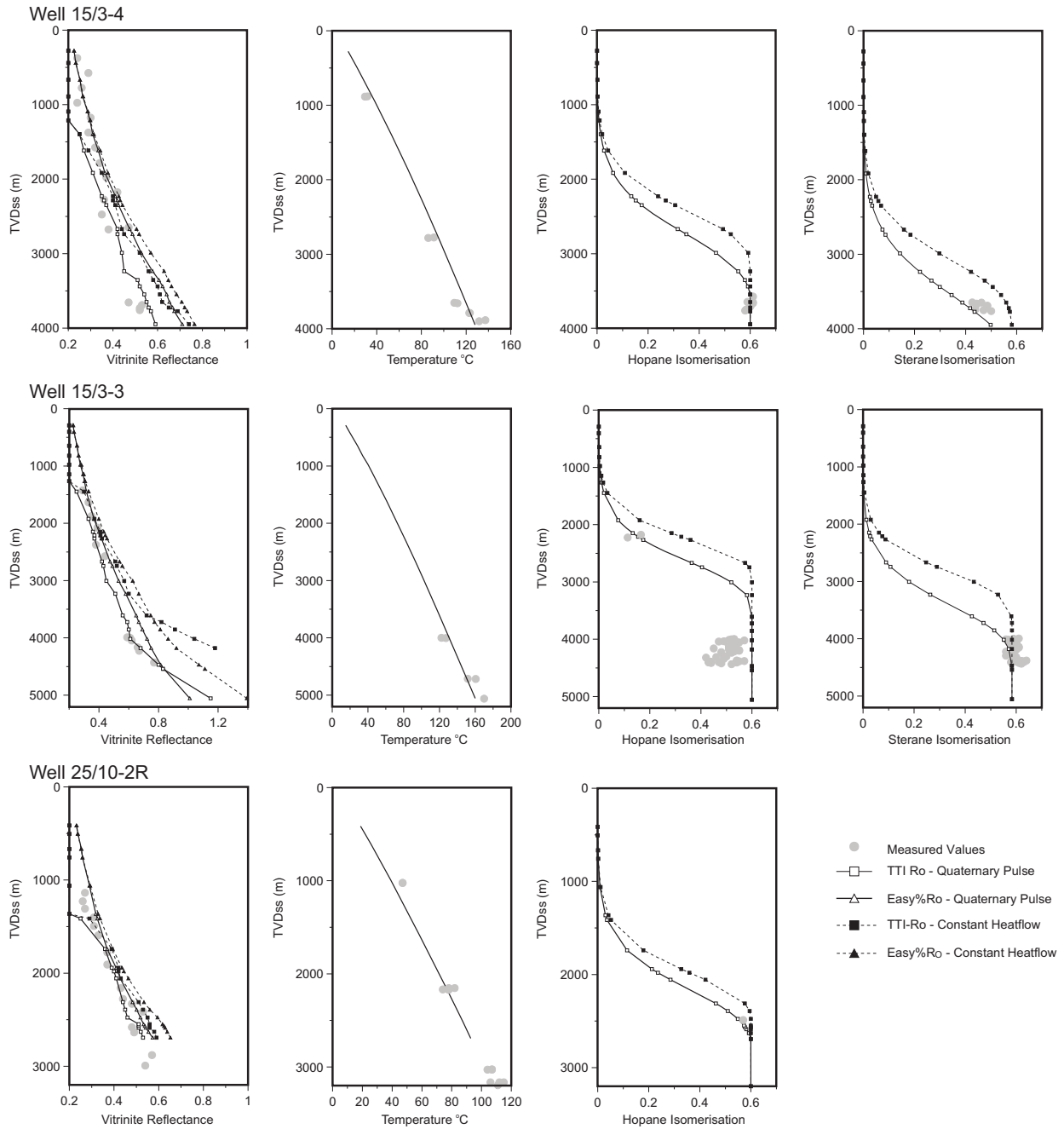
Fig. 6. Measured (grey circles) and modelled temperature, vitrinite reflectance, hopane and sterane isomerisation depth plots for three wells illustrating calibration of the 1D models. For each well, results for two heatflow scenarios are shown. Scenario one (full line) includes a recent heatflow pulse to match present day temperatures, while scenario two (stippled line) uses a constant heatflow in the Tertiary to match present day temperatures. All 1D sites have been calibrated using vitrinite reflectance calculated with a modified TTI-Ro approach (squares), but Easy%Ro vitrinite reflectance (Sweeney and Burnham, 1990) has been calculated in addition for comparison (triangles). Best match to the observed data is achieved using TTI-Ro and scenario one.

hot fluids. Burley (1993) argued that hot fluids expelled from the deep graben centre are responsible for this effect and that this fluid flow drive was initiated during the early Tertiary.

3.2.5. Kinetics

Hydrocarbon generation was modelled using compositional kinetics schemes which divide the bulk hydrocarbon fraction generated into four boiling point fractions. These pseudo-components include heavy oil (C_{15+}), light oil (C_{6-14}), wet gas (C_{2-5}) and dry gas (C_1). Since the Upper Jurassic Draupne and Heather Formation are very important source rocks in the North Sea area, a large number of studies deal with the kinetics of hydrocarbon generation from
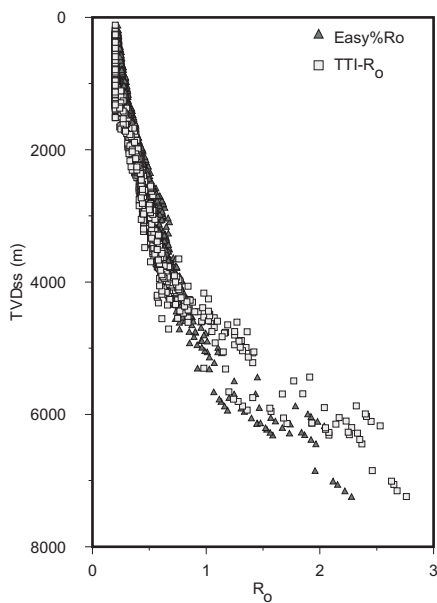
Fig. 7. Regional modelled vitrinite reflectance depth trend. Values calculated using the TTI-Ro relationship tend to be slightly lower than values calculated using the Easy%Ro algorithm (Sweeney and Burnham, 1990) down to about 4200 m and higher below.

these source rocks (e.g. Espitalié et al., 1988; Burnham and Dahl, 1993). Generation from Upper Jurassic source rocks in events 6, 7 and 8 has been modelled using a kinetic scheme after Burnham and Dahl (1993) and Dahl and Meisingset (1996). Although it was not possible to check the compositional yields, the bulk kinetics were validated by comparison of modelled transformation ratios with transformation ratios for the upper and lower Draupne as well as the Heather Formation calculated from Rock-Eval data in Justwan et al. (2005). Figure 8 shows that modelled and observed data are in reasonably good agreement, only generation in the low maturity range is slightly overestimated compared to the data of Justwan et al. (2005). Using one kinetic scheme for the modelling of hydrocarbon generation from all three Upper Jurassic source rock units is of course a simplification. The differences in transformation ratios based on Rock-Eval data in Justwan et al. (2005) and the work of Keym et al. (2006), which showed significant variations in petroleum kinetics as a result of facies variations, indicate that the use of different kinetic models for each of the Upper Jurassic source rocks might have improved modelling accuracy further.

Modelling hydrocarbon generation from Middle Jurassic strata emerged to be more difficult. The models of Espitalié et al. (1988) and Behar et al. (1997) for Brent coals and the kinetic schemes of Burnham (1989) and Burnham and Sweeney (1989) for Type III kerogen have been evaluated. Comparison of bulk transformation ratios for the Middle Jurassic based on Rock-Eval data (Justwan et al., 2005) with modelled transformation ratios (Fig. 9) indicates that the kinetic schemes of Burnham and Sweeney (1989) and Espitalié et al. (1988) fit the observed data best. The transformation ratios based on Burnham (1989) overestimate hydrocarbon generation in the range above 1 % Ro (Fig. 9), while the model of Behar et al. (1997) significantly underestimates hydrocarbon generation. Since the model of Espitalié et al. (1988) offers a four component kinetic scheme, it was chosen to model hydrocarbon generation from Middle Jurassic sources in the South Viking Graben. Effects of the differences in the range of the boiling point fractions of Espitalié et al. (1988) (C_{6-15}) to the ones used in the model (C_{6-14}) were considered negligible.

3.3. Pseudo-3D modelling

3.3.1. Structural framework

After development of the conceptual input model and subsequent 1D simulation of the geohistory of 38 well sites and 8 pseudo-well sites, the map-based pseudo-3D model was built in the *BasinAssist* module of the mapping software *IRAP*®. Model input and simulation data were for this
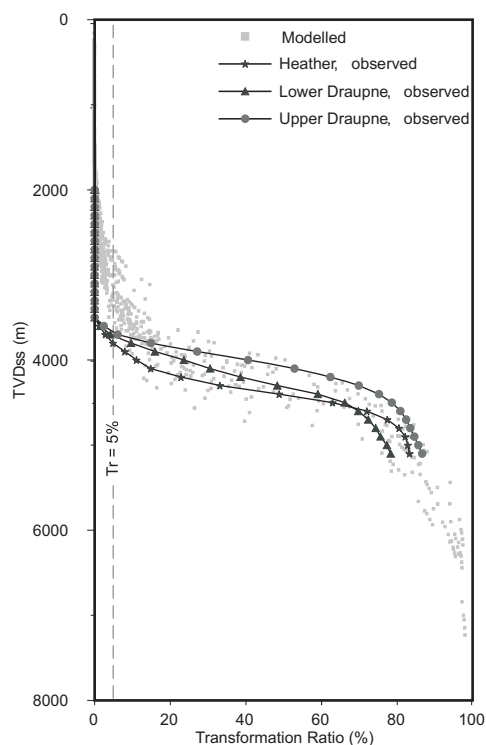

Fig. 8. The bulk kinetic model for the Upper Jurassic was taken from Burnham and Dahl (1993) and validated by comparison of modelled transformation ratios for wells and pseudo-wells with empirically determined transformation ratios from Justwan et al. (2005). Modelled and observed data match well below 4000 m, but the kinetic model slightly overestimates generation in the shallower section.
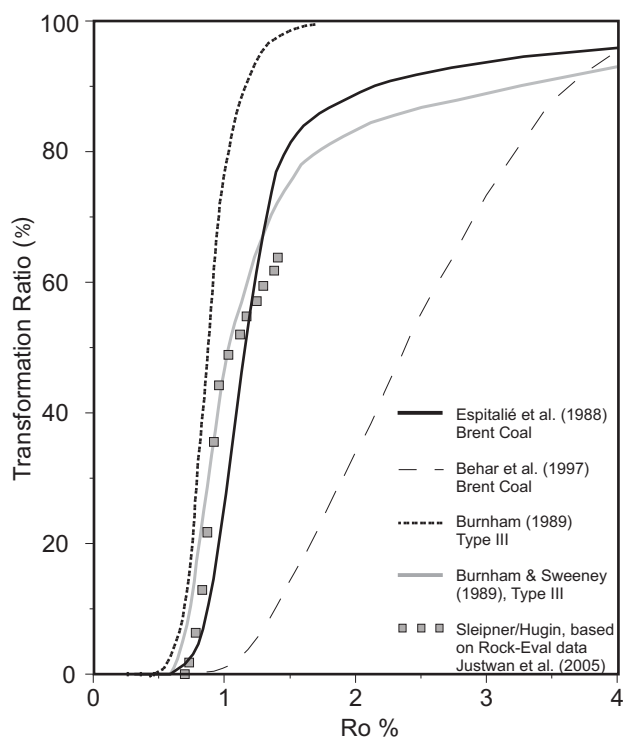
Fig. 9. Comparison of bulk modelled transformation ratios for the Middle Jurassic using different kinetic models from Behar et al. (1997), Burnham (1989), Burnham and Sweeney (1989) and Espitalié et al. (1988) with transformation ratios based on Rock-Eval data from Justwan et al. (2005). The model of Espitalié et al. (1988) fits the observed data and was selected for modelling of kerogen transformation of the Middle Jurassic source rocks.

purpose collected in *BASXYZ*, the simulation database (Fig. 2). A 3D structural framework was set up from depth maps used earlier (Fig. 3), and missing maps have been generated using the grid interpolation routine in *IRAP*[®] (Dahl and Meisingset, 1996). Once the 3D structural framework was set up, structural reconstruction at all 36 reference ages was performed. Structural reconstruction is essential for accurate estimation of source rock burial depths at specific times as well as for determination of migration pathways. Reconstruction was achieved by removal of all layers above the respective surface and adjusting paleo-water depths to the appropriate level at the time step. Water depth maps have been generated from Kyrkjebø (1999), and missing maps were interpolated between existing maps. Subsequently, the remaining layers were decompacted.

3.3.2. Calculation of generated hydrocarbon masses

The first step in the assessment of timing of generation and the determination of generated hydrocarbon mass is the mapping of the kerogen transformation ratios for the four pseudo-components for all reference ages and source events in *IRAP*[®]. Transformation ratio maps are created in a two step process. Cross-plotting of transformation ratios for the four model pseudo-components and vitrinite reflectances (Easy%Ro) shows a strict curvilinear relationship (Fig. 10) that can be used to create transformation ratio maps from maps of vitrinite reflectance. Even though all 1D models have been optimised with TTI-Ro, modelled Easy%Ro can be used in this process since this is only an intermediate step. The required vitrinite reflectance maps were created in *IRAP*[®] from modelled data. A regional vitrinite reflectance-depth relationship and reconstructed depth maps of the horizon at the desired time step were employed to interpolate between data points. In the next step, a kriging approach with external drift is employed to map transformation ratios using the transformation ratio-vitrinite reflectance
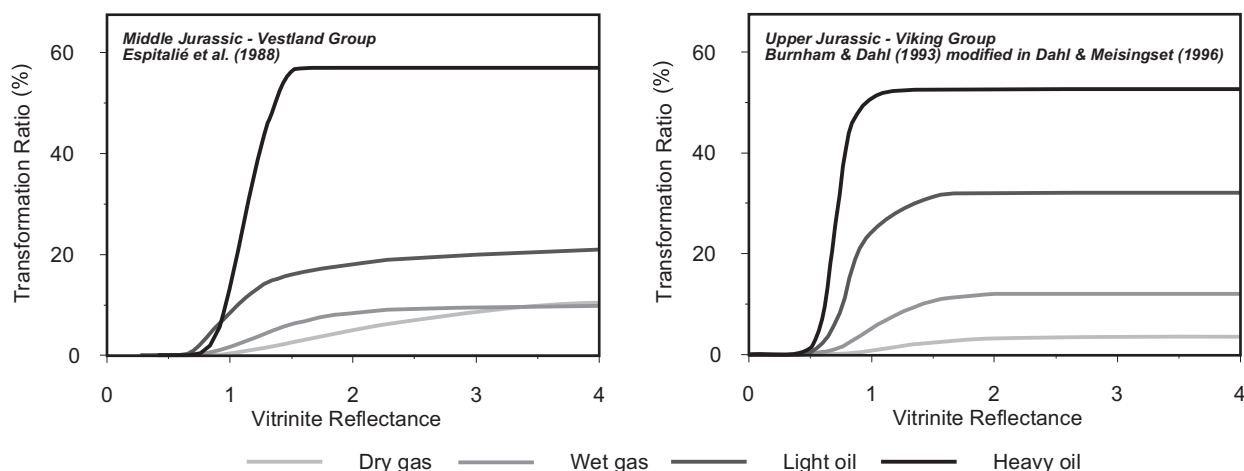

Fig. 10. Compositional yield curves (Tr - Easy%Ro) for the two kinetic models used in this study. Generation from Middle Jurassic source rocks was modelled using the model of Espitalié et al. (1988), while the yield curves for the Upper Jurassic are based on the kinetic scheme of Burnham and Dahl (1993) modified in Dahl and Meisingset (1996).

relationship established earlier (Fig. 10). This rapid mapping approach yields geologically sound maps honouring the structure of the basin and is superior to contouring transformation ratios directly from 1D model results, which is associated with large uncertainties due to the small number of data points.

Incremental generated and expelled hydrocarbon masses were calculated based on transformation ratio maps at 28 time steps as well as the source rock potential and thickness maps. Primary and secondary cracking was calculated using algorithms and stoichiometric coefficients after Braun and Burnham (1992). Expulsion was simulated using a simple saturation controlled expulsion model. Upper Jurassic source rock quality and thickness was taken from Justwan et al. (2005), but isochores have been corrected to true shale thicknesses using sand/shale distributions from well logs. The set of source rock quality maps used (Justwan et al., 2005) contains separate maps for gas-prone and oil-prone TOC within the respective formation. The oil-prone fraction of organic matter, TOCII, is converted into light and heavy oil, while TOCIII, the gas-prone active fraction, generates dry and wet gas.

The Middle Jurassic event 5 comprises sands, shales, coals and carbargillites of variable thickness and geochemical properties, and had therefore to be modelled as a bulk unit. This has been achieved by mapping shale and coal thicknesses from well logs and the map of Field (1985) and assigning both rock types average maturity corrected TOC and HI values from our Rock-Eval database, 62 wt% TOC and 260 g HC/kg C_{org} HI for coals and 7 wt% TOC and 230 g HC/kg C_{org} for shales. This information was used together with maps of the average sand thickness (TOC = 0 wt%) to create an average bulk Middle Jurassic TOC map. TOC for these maps is converted in the model into all four modelled components.

3.3.3. Expulsion

Mechanisms of expulsion of hydrocarbons from the source rock are still subject to debate: Expulsion has been simulated previously by basin scale compaction and Darcy flow modelling (e.g. Ungerer et al., 1990), application of bulk saturation thresholds (e.g. Forbes et al., 1991) and as a function of absorption and adsorption within the kerogen (Sandvik et al., 1992; Pepper and Corvi, 1995; Ritter and Grøver, 2003). Expulsion in *IRAP*®/*BasinAssist* was modelled using a saturation threshold approach to expel hydrocarbons once a saturation threshold (kg HC/t rock) has been surpassed.

When modelling generation of hydrocarbons in a multicomponent approach, fractionation processes have to be considered during expulsion. In general, expulsion efficiencies for gas are high and can reach nearly 100 % (Leythäuser et al., 1982), while efficiencies for oil reach about 60-90 % (Cooles et al., 1986). In addition, compounds are reported to be released in the order n-alkanes – branched alkanes – aromatics – resins – polars – asphaltenes (Pepper and Corvi, 1995). Calibration of saturation thresholds for the four boiling point fractions modelled in this study has to be done ultimately to match observed hydrocarbon quality in reservoirs. This is beyond the scope of this regional study and a subject for follow-up prospect evaluation studies. The starting point for calibration of the expulsion model were the *IRAP*® default settings, assuming decreasing expulsion efficiencies in the order dry gas – wet gas – light oil – heavy oil. Calibration was attempted by comparison of modelled residual saturation (C_{6+}) and measured values (S1 from Rock-Eval). Limitation of this technique is that only oil expulsion can be calibrated since the S1 peak does not contain gaseous components and the modelled C_{6+} fraction and observed S1 are not fully equivalent (Ungerer, 1993). The threshold values for heavy and light oil have been adjusted to match modelled retained light and heavy oil and measured S1 values (Fig. 11a). Since individual calibration for the respective boiling point fractions was not possible, the relative proportions of the default thresholds were kept. Five cases (Fig. 11, Table 1) have been modelled in order to determine appropriate saturation thresholds. As discussed in Justwan et al. (2005), expulsion from Upper Jurassic sources begins at depths of about 4000 m in the area (Fig. 11a). Case 3 fits the observed data best and was chosen for detailed modelling of hydrocarbon expulsion. As Figure 11b shows, the chosen expulsion model yields only 75 % of the total heavy oil generated (Case 1). Raising expulsion thresholds also increases the proportion of gas in the total yield since more oil is retained and cracked to gas (Fig. 11b).
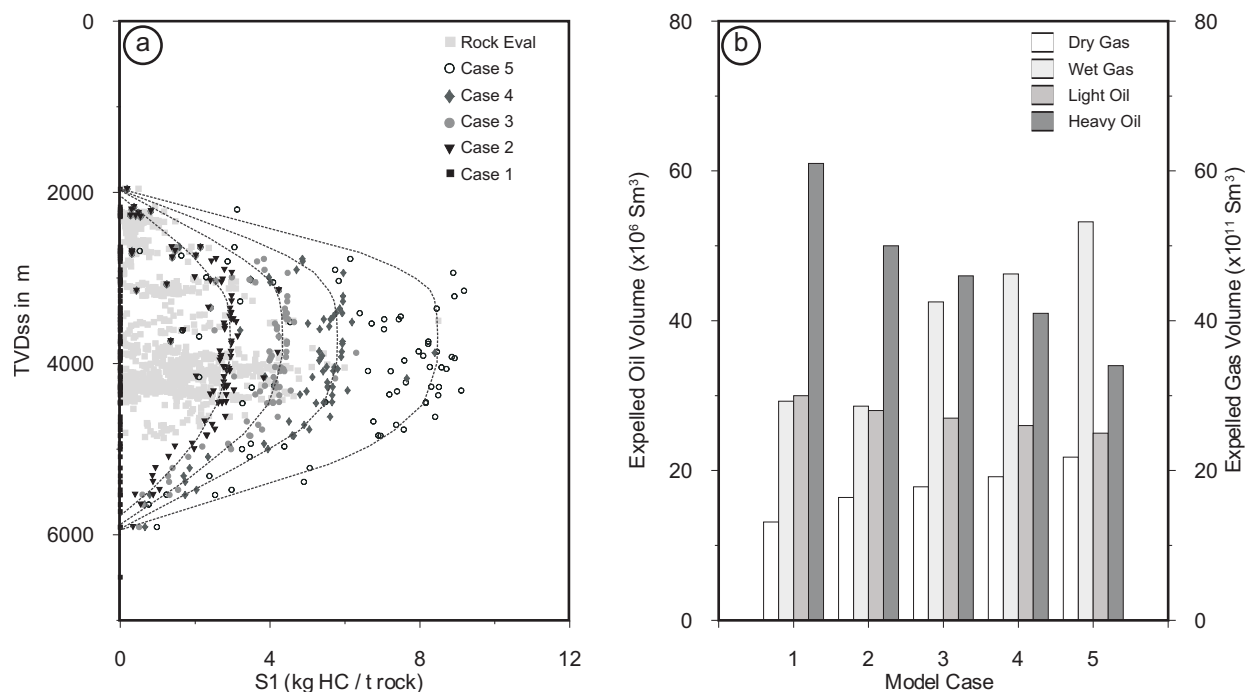
Fig. 11. Comparison of modelled residual saturation (C_{6+}) for the Upper Jurassic for five modelled cases with measured S1 from Rock-Eval (a) and resulting modelled hydrocarbon volumes (b). Although modelled and observed S1 are not fully equivalent (Ungerer, 1993), this comparison offers a good means of calibration of the expulsion model used. Five cases with different saturation thresholds in the expulsion model were simulated (Table 1). Case 3 appears to fit the observed data best and was selected. This case represents a "middle case" as expelled oil and gas volumes are between the extreme values of cases 1 and 5.

Modelling expulsion from Middle Jurassic source rocks is difficult. Experiments indicate that coals are able to generate significant amounts of C_{6+} compounds (e.g. Espitalié et al., 1988; Behar et al., 1997). Justwan et al. (2006) and Isaksen et al. (2002) have demonstrated the coal origin of light oils and condensates in the Sleipner area. But the overwhelming majority of liquid hydrocarbons in the South Viking Graben derives from Upper Jurassic shaly source rocks (Justwan et al., 2006). The discrepancy between the observed oil and gas volumes and experimental data is explained by retention of hydrocarbons in the source rock (e.g. Sandvik et al., 1992; Behar et al., 1997; Ritter and Grøver, 2003). Since sophisticated adsorption models for retention in coal, such as in Ritter and Grøver (2003), are beyond the scope of this project and beyond the capabilities of the software used, the problem is approached by raising saturation thresholds for heavy and light oil. The observed situation in the South Viking Graben, where liquid hydrocarbons sourced from the Middle Jurassic are only encountered south of 58°40' (Justwan et al., 2006), can be

simulated by raising thresholds up to 7.5 and 5.5 kg HC/t rock for heavy and light oil respectively from Case 3. These assumptions and the fact the Middle Jurassic was treated as a bulk unit including sands, shales and coals make a calibration as shown in Figure 11 for the Upper Jurassic impossible.

The following detailed discussion of the modelling results (section 4) is based on Case 3 for the Upper Jurassic and the expulsion model explained above for the Middle Jurassic.

Table 1
Saturation thresholds (kg HC/t rock) for the expulsion model used in the five modelled cases

Model Case	C_1 Dry Gas	C_{2-5} Wet Gas	C_{6-14} Light Oil	C_{15+} Heavy Oil
1	0	0	0	0
2[a]	0.65	0.36	0.2	0.13
3	0.98	0.54	0.3	0.2
4	1.3	0.72	0.4	0.26
5	1.95	1.08	0.6	0.39

[a] default settings in *BasinAssist*

3.3.4. Secondary migration

Several secondary migration processes have been invoked for the South Viking Graben. Reservoir units in close proximity to the source rock, e.g. the intra Draupne Formation sands of the Brae and Gudrun area, are charged by very short distance migration (Cornford, 1998; Kubala et al., 2003). Long distance vertical migration is proposed for the Frigg area in the north (Goff, 1983; Cornford, 1998; Kubala et al., 2003), while the Sleipner area in the south is charged through up-flank long distance migration through extensive sandstone units (Isaksen et al., 2002; Kubala et al., 2003). One process which still remains poorly understood is the migration from Jurassic source rocks into the Tertiary (Johnson and Fisher, 1998), although now most authors agree on a general mechanism. This includes a basin to margin pathway within Jurassic carriers and vertical leakage into the Tertiary at fault zones at the western margin of the Utsira High followed by migration within the Tertiary system (Barnard and Bastow, 1991; Isaksen and Ledje, 2001; Kubala et al., 2003). It would therefore be desirable to use maps displaying fault traces as

Table 2
Drainage polygons used in this study and associated hydrocarbon accumulations

Drainage Polygon	Major Fields/Discoveries in Polygon [a]
I	Odin, Frigg, Lille Frigg, 25/2-10S
II	Skirne, Byggve, 25/6-1, Heimdal, Frøy, Lille Frøy, Vale, 25/5-5, Vilje
III	Jotun, Alvheim, Peik, 24/9-5
IV	Balder, Ringhorne, Grane
V	Gudrun, East Brae (UK)
VI	Glitne, Dagny, Miller (UK), Kingfisher (UK)
VII	Sleipner Øst/Vest, Gungne, Sigyn, Volve, Loke
VIII	Varg, 6/3-1, Cyrus (UK), Andrew (UK), Moira (UK), Fleming (UK), Hawkins (UK), Maureen (UK)

[a] If not indicated otherwise: Norwegian sector

well as 2 horizons within the Jurassic and in the Tertiary for a comprehensive evaluation of secondary migration pathways, as suggested by Barnard and Bastow (1991) and Kubala et al. (2003).

Since maps of fault traces were not available for this study and the Middle Jurassic sands are often regarded as the main migration conduits (Miles, 1990), the top of event 5 was chosen as the horizon to determine drainage polygons for the region. The polygons were determined manually using orthocontour maps of this horizon at 5 time steps (0 Ma, 12 Ma, 28.5 Ma, 46 Ma and 61 Ma) to honour changes in basin configuration over time. Changes in basin configuration affect mostly the adjacent Stord Basin and drainage towards the Norwegian mainland, whereas the configuration of the deep basin area remains largely unaffected. In addition, it has been observed that the crest of the Utsira High slightly shifts to the east during the Paleocene and Oligocene. The model uses available drainage areas at each time step and, if not available, the next younger drainage area set.

This study is regional and, due to the lack of detailed maps with fault traces and the complex migration in the area, drainage areas have not been created for each field but rather represent "mega drainage areas" charging subareas or field clusters (Table 2).

4. Modelling results

4.1. Depth of the hydrocarbon generation window

Modelling shows that oil generation for Upper Jurassic source rocks ($Tr_{Oil} = 5\%$) commences at 0.56 % Ro at a depth of about 3500 m, and transformation ratios of 90 % are reached at 1.02 % Ro at a depth of approximately 4800 m. The main phase of gas generation for the Upper Jurassic source rocks ($Tr_{Gas} = 5\%$) begins at 0.66 % Ro at depths of about 3800 m and ends ($Tr_{Gas} = 90\%$) at 1.65 % Ro around 5700 m depth. Due to different generation kinetics, the generative windows for oil and gas ($Tr_{Oil/Gas} = 5\text{-}90\%$) are at different depths and maturities for the Middle Jurassic source rocks. The oil window ranges from 0.87 % to 1.96 % Ro and 4400 to 6300 m, while the gas window is entered at 0.88 % Ro and 4400 m depth. The base of the gas window for the Middle Jurassic source rocks has not been encountered in the modelled wells.

4.2. Timing of hydrocarbon generation and expulsion

Detailed knowledge of the subsidence history in the area is necessary in order to understand and predict timing of hydrocarbon generation. Five characteristic periods can be identified after source rock deposition in the Middle and Upper Jurassic (Fig. 12). The Lower Cretaceous is characterised by low subsidence rates in the entire study area with very little sediment being deposited (Fig. 4, 12). Onset of rapid subsidence occurred in the Upper Cretaceous at
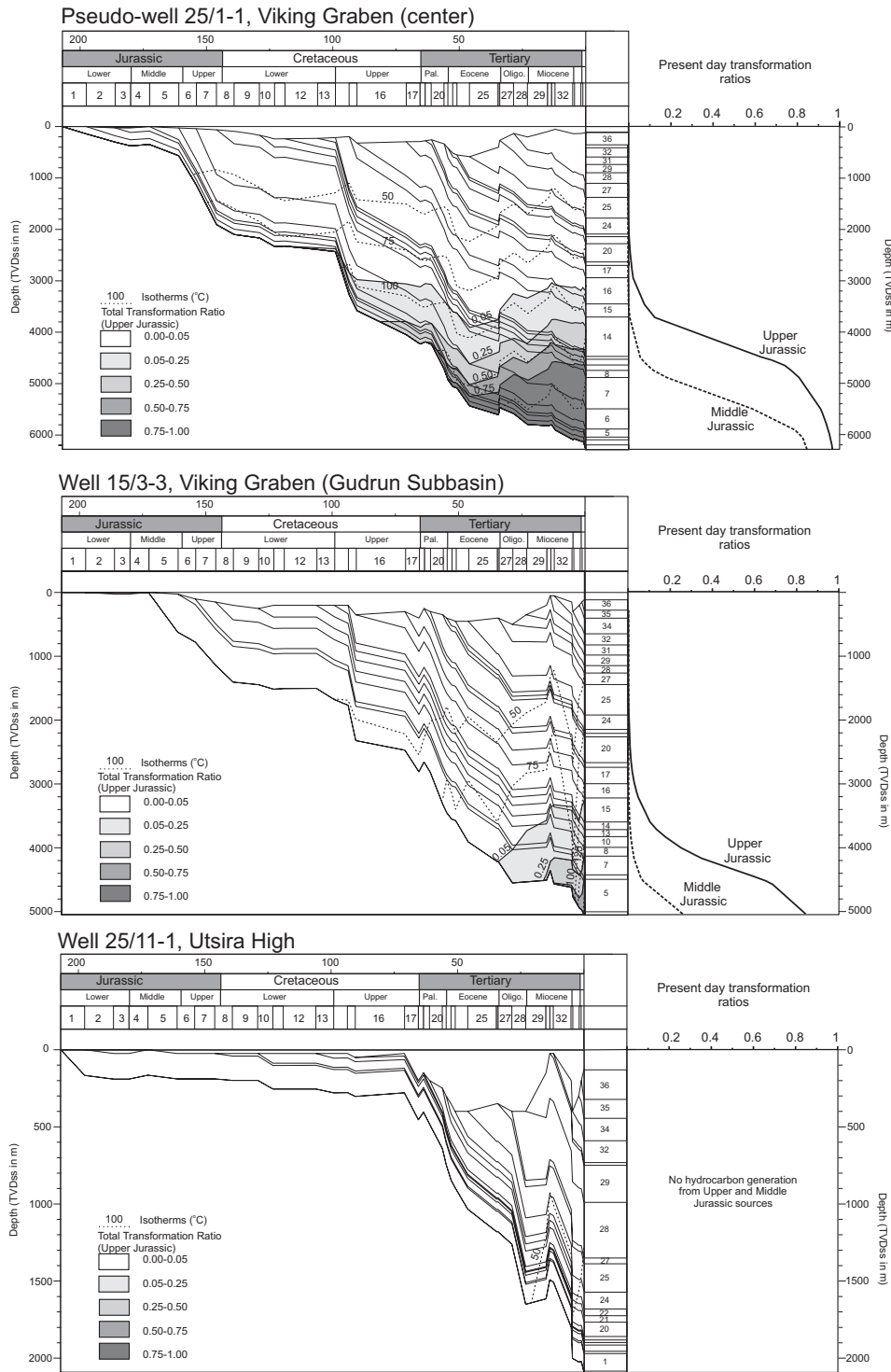
Fig. 12. Geohistory plots for three wells in the South Viking Graben (locations see Fig. 1) showing temperature and transformation ratio development (for Upper Jurassic source rocks only) as well as present day transformation ratios versus depth (Upper and Middle Jurassic source rocks). While the upper Draupne Formation (event 8) has reached transformation ratios above 0.75 at present day in the deep part of the Viking Graben (Pseudo-well 25/1-1), the Gudrun Subbasin (Well 15/3-3) has not reached peak oil generation yet, and the Utsira High (Well 25/11-1) shows no hydrocarbon generation.

around 90 Ma above the buried graben, while the Utsira High area to the east received little or no sediment (Fig. 12). Regional uplift of the East Shetland Platform caused very high subsidence rates in the early Tertiary (Ziegler, 1990; Nadin and Kusznir, 1995; Kubala et al., 2003) (Fig. 12). Shallowing of the basin in the Miocene led to reduced subsidence. This phase was followed by a period of renewed subsidence related to the glaciations in the Quaternary. The following section will illustrate how closely timing of hydrocarbon generation is related to these episodes.

In the following text, several terms specifying locations are used for simplification. Drainage polygons as described in Table 2 and the "main graben area", comprising the Beryl Embayment, Fensal-, Volve-, Vilje-, Vana-, and Ve-Subbasins, the Fisher Bank Basin as well as the Frigg and Andrew Ridge and deepest sections of the Heimdal High, Gudrun Terrace and the East Shetland Basin (Fig. 1), are used. Source rocks have not reached maturity in the entire study area (Fig. 13), although source rock deposition occurred in a much wider area (Justwan et al., 2005). In general, only the "main graben area" has entered the generative window, while the flanks and the highs such as the Utsira High remain immature. The only exceptions are the Bjørgvin arch and the western flank of the Stord Basin in Blocks 25/3 and 26/4 (Fig. 13)

Kerogen transformation (Tr = 5 %) commenced as early as in the Lower Cretaceous (110 Ma) for the Middle Jurassic source rocks in the deepest patches in the South Viking Graben in Block 24/9. The major parts of the main graben area, however, entered the hydrocarbon generation window mostly in the Paleogene between 60 and 20 Ma (Fig. 13a). The modelling interestingly shows that only the deepest sections of the graben have generated hydrocarbons, while the rest of the main graben area remains immature. The Middle Jurassic source rocks have in large areas, especially within drainage polygons VII and VIII, never experienced the onset of kerogen transformation. The Heather Formation has surpassed 5 % kerogen transformation in a much wider area than the Middle Jurassic source rocks due to the different kinetics used and entered the hydrocarbon generation window in large areas already in the Lower Cretaceous. In these deep sediment sinks of the graben, Upper Jurassic and lowermost Cretaceous subsidence rates and sediments supplies were high and led to rapid burial and early maturation of the Heather Formation. In the shallower sections of the main graben, the Heather Formation reached 5 % kerogen transformation in the Paleocene to Oligocene between 65 and 23.5 Ma (Fig. 13b). The onset age of hydrocarbon generation for the lower Draupne Formation was in the Upper Cretaceous (100 Ma) in the deepest part of the graben in polygon I (Fig. 13c). The major part of the main graben area entered the hydrocarbon generative window in the Paleocene to Oligocene. The youngest and shallowest unit, the upper Draupne Formation, started hydrocarbon generation earliest in the Paleocene, while the major part of the main graben area reached levels of 5% transformation ratio in the Eocene to Middle Miocene (55 to 10 Ma) (Fig. 13d). As observed for the Middle Jurassic, modelling results also indicate late onset of hydrocarbon generation for the Upper Jurassic kitchen in polygons VII and VIII. The fact that the Upper and Middle Jurassic source rocks in the largest part of the South Viking Graben commenced hydrocarbon generation in the early Tertiary is related to the onset of rapid subsidence during that period as illustrated in Fig. 12.

Mapping of present day transformation ratios (Fig. 14) shows that the Middle Jurassic source rocks have not at present realised their entire hydrocarbon potential in the main graben area. Large parts of the Greater Frigg Area in the north (polygons I and II) as well as polygons III and IV show transformation ratios well above 70 %, but large areas in the south remain immature or at ratios below 30 %, especially in polygons VII and VIII (Fig. 14a). In contrast, the Heather Formation as well as the lower Draupne Formation have reached higher levels of kerogen transformation due to faster reaction kinetics compared to Middle Jurassic source rocks. The Heather Formation has exhausted its hydrocarbon potential in very large areas in the main part of the graben (Fig. 14b). The lower Draupne has realised most of its hydrocarbon potential, although not to the same extent as the Heather Formation (Fig. 14c). In particular, the deep kitchen areas in polygon I to IV have reached transformation ratios above 80 %. The shallowest and youngest source rock unit, the upper Draupne Formation, has only reached transformation ratio levels above 70 % in the northern- and southernmost parts of the study area (Fig. 14d), while the major parts remain well below this value. The upper Draupne Formation is the richest and most oil-prone source rock unit (Justwan et al., 2005) but is not fully mature in the entire main graben area. The results also indicate that parts of the Bjørgvin Arch and the flank
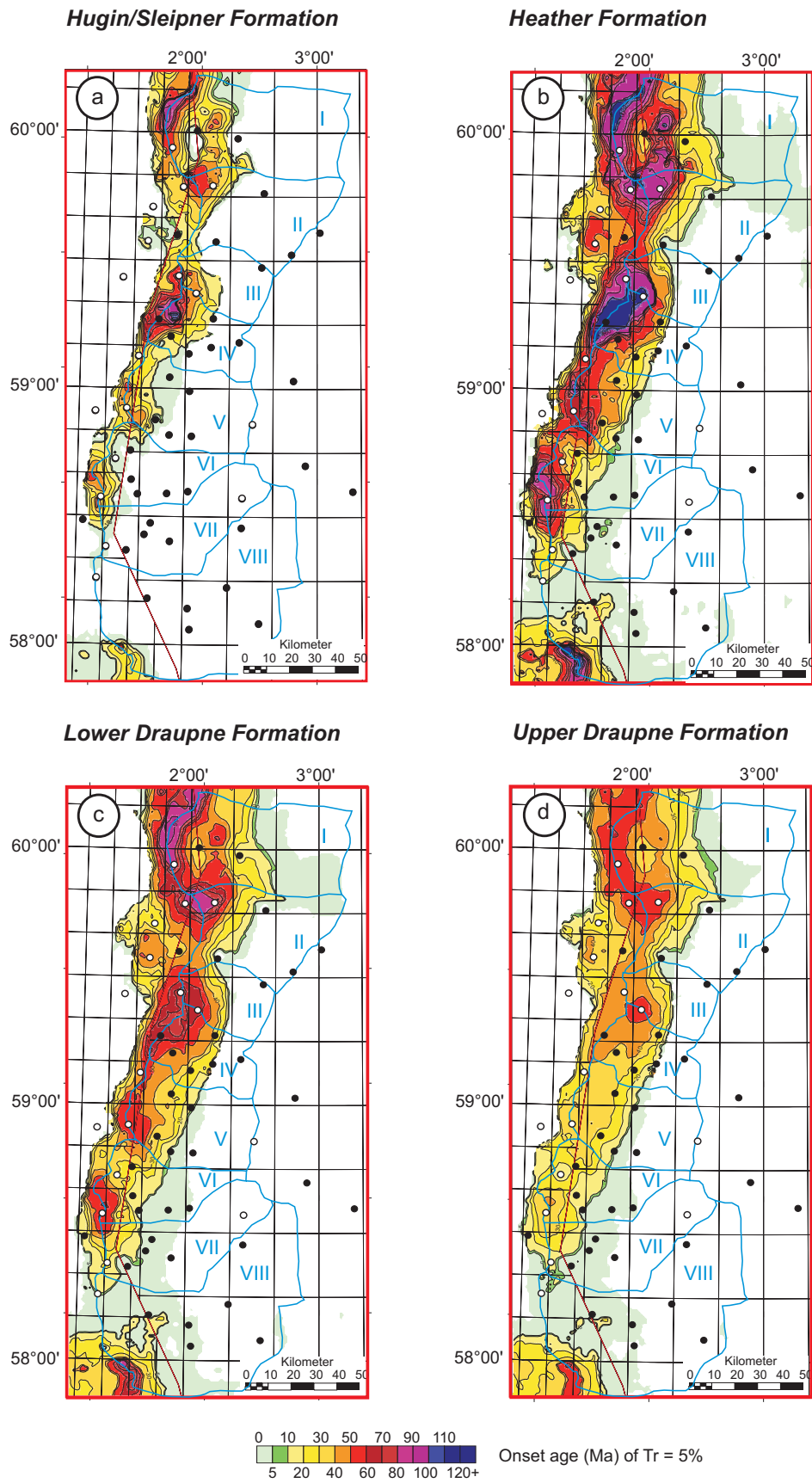
Hugin/Sleipner Formation

Heather Formation

Lower Draupne Formation

Upper Draupne Formation

Fig. 13. Onset age in Ma for transformation ratios of 5 % displayed for the (a) Middle Jurassic (b) Heather Formation (c) lower Draupne Formation and (d) upper Draupne Formation. Locations of modelled wells are indicated by full circles, empty circles indicate pseudo-well locations. Blue outlines delineate drainage polygons (see Table 2).

of the Stord Basin (Blocks 25/3 and 26/4) have just entered the hydrocarbon generative window for the Upper Jurassic source rocks (Fig. 14b, c, d).

Upon closer examination of the expelled volumes, two distinct phases of hydrocarbon expulsion can be observed. These phases were caused by high subsidence rates in the early Tertiary, followed by reduced subsidence in the Miocene and renewed subsidence in the Quaternary (Fig. 15). The main phase of hydrocarbon expulsion from Upper Jurassic source rocks in the South Viking Graben lasted from 61 to 15 Ma with peak expulsion in the Lower Miocene (23-15 Ma), although minor initial hydrocarbon expulsion is observed before (Fig. 15). This phase was followed by a period of reduced expulsion related to the shallowing of the basin, and renewed expulsion in the Quaternary (2-0 Ma) related to the rapid subsidence during this period. Major expulsion from Middle Jurassic source rocks began at 51 Ma in the Eocene for gas and, due to the expulsion model used, later for oil in the Lower Miocene (23 Ma). Renewed expulsion in the Quaternary is also evident from Middle Jurassic sources.

The second phase in the Quaternary becomes increasingly more important in the south of the study area (e.g. Fig. 15g). In the southern half of the study area, Quaternary subsidence rates were high, enough to move the source rocks which were only buried at shallow depth before the Quaternary into the hydrocarbon generation window.

4.3. Volumes of hydrocarbons generated and expelled

Calculated hydrocarbon masses were converted into hydrocarbon volumes at surface conditions using formation volume factors of 1 and a density of 0.85 g/cm^3 for heavy oil, 0.75 g/cm^3 for light oil, 0.0017 g/cm^3 for wet gas and 0.00071 g/cm^3 for dry gas. Modelling suggests a total of 74198 x 10^6 Sm^3 of oil expelled from Upper and Middle Jurassic sources, while 8218 x 10^9 Sm^3 of gas have been expelled from all source rock horizons (Table 3, Fig. 16). The most oil-prone area is the kitchen in drainage polygon IV with 16975 x 10^6 Sm^3 oil expelled with the major contribution from the lower Draupne Formation (Table 3, Fig. 16). Model results agree with field observations, since the source kitchen in polygon IV charges the biggest oil fields in the area, Balder, Ringhorne and Grane whose reservoired hydrocarbons have been correlated to the Draupne Formation (Justwan et al., 2006). The source kitchen in drainage polygon I also yields significant amounts of oil. In contrast, the main graben area in polygons VII and VIII contains large areas that do not yield hydrocarbons, as Figure 16 shows. The low amounts of oil generated in polygons VII and VIII suggest that sufficient generation is a risk factor for future exploration in these areas. The major contribution of oil is from the lower Draupne Formation (Fig. 17) since 54 % of all oil expelled is sourced from this source rock unit. The upper Draupne Formation contributes 24 %, while the Hugin and Sleipner Formations contribute 0.5 %. It has been shown earlier that the upper Draupne Formation is the most oil-prone unit and the lower Draupne Formation contains high amounts of gas-prone material (Isaksen and Ledje, 2001; Justwan and Dahl, 2005; Justwan et al., 2005), but modelling clearly indicates that the lower Draupne Formation contributes most of the oil due its higher degree of maturation and greater thickness. Justwan et al. (2006) identified Heather sourced hydrocarbons only in drainage polygon II in Pre-Jurassic reservoirs, although modelling suggests that the Heather Formation sourced 21.5 % of the total oil amount in the area. This can also be explained by the modelling results since the contribution of Heather sourced oil in polygon II amounts to 44 %, the highest percentage in all drainage polygons. In other areas, such as polygon IV, Heather sourced hydrocarbons might contribute to the total reservoired hydrocarbons, but the geochemical signature of the more abundant Draupne Formation sourced oil will dominate in the mixtures. Although the Upper Jurassic source rocks have surpassed 5 % kerogen transformation on the Bjørgvin Arch and the western flank of the Stord Basin (Fig. 14), hydrocarbon generation is insignificant (Fig. 16) due to the relative immaturity and small thickness of the source rocks.

The second phase of hydrocarbon generation in the Quaternary is of great volumetric importance. Over 11 % of all oil is expelled in the Quaternary during events 35 to 36. This late phase of oil charge could be responsible for late charge of structures and dilution of oils from previous charge phases.

Hugin/Sleipner Formation

Heather Formation

Lower Draupne Formation
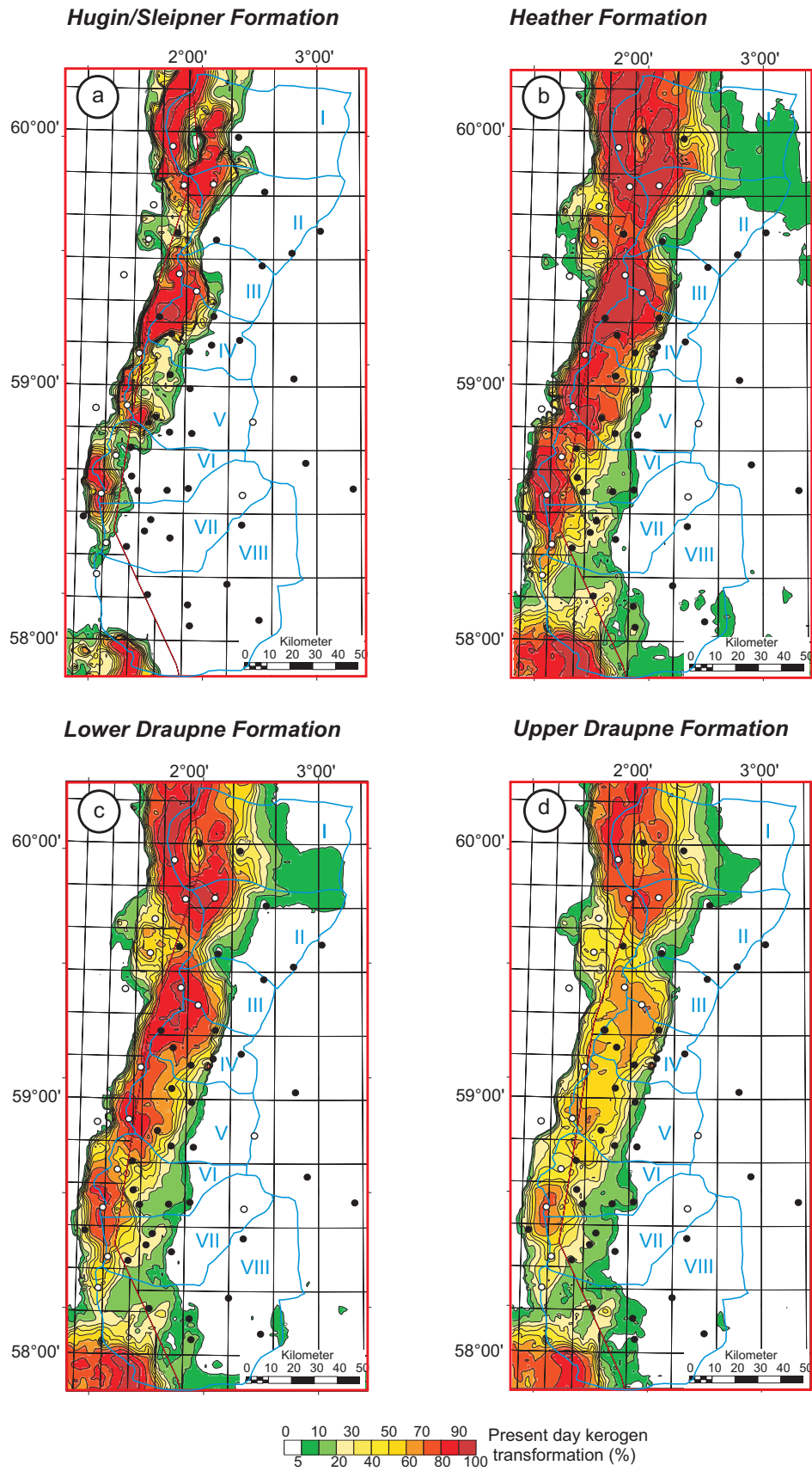
Upper Draupne Formation

Fig. 14. Present day transformation ratio (%) displayed for the (a) Middle Jurassic (b) Heather Formation (c) lower Draupne Formation and (d) upper Draupne Formation. Locations of modelled wells are indicated by full circles, empty circles indicate pseudo-well locations. Blue outlines delineate drainage polygons (see Table 2).
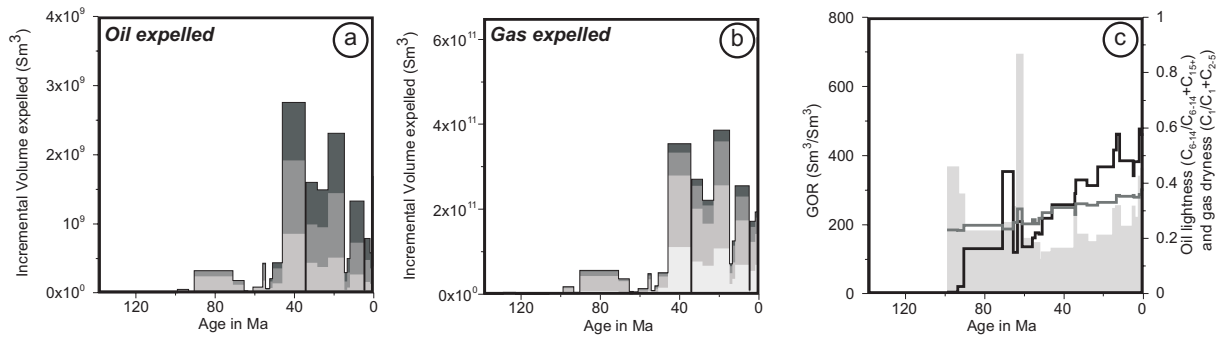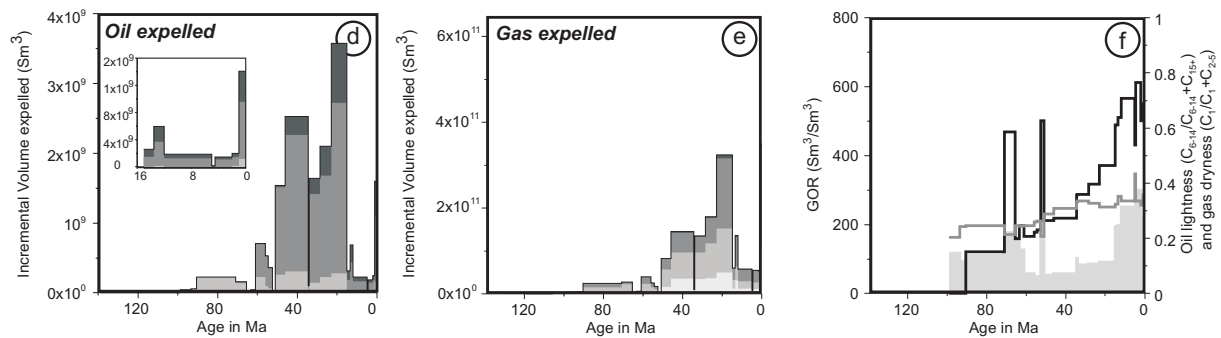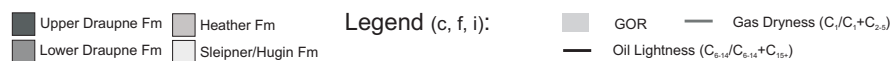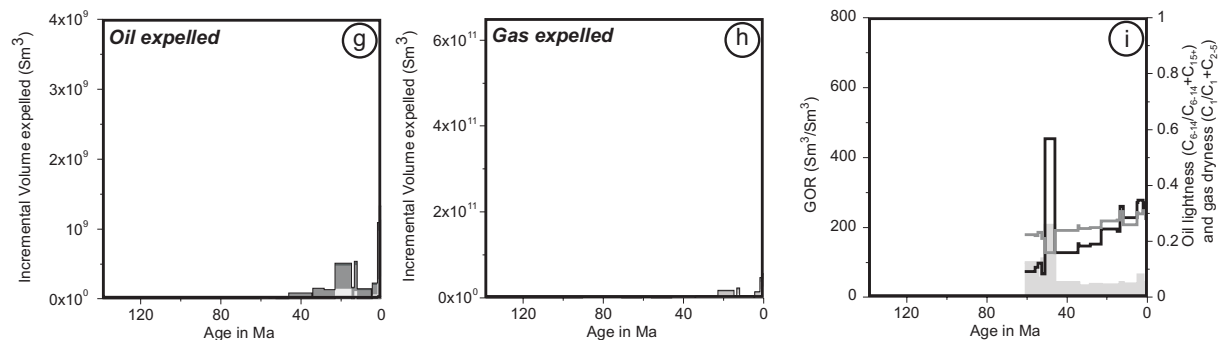
Drainage Polygon I

Drainage Polygon IV

Drainage Polygon VII

Fig. 15. Incremental oil and gas volumes expelled through time as well as change in GOR, gas dryness (C_1/C_1+C_{2-5}) and oil "lightness" ($C_{6-14}/C_{15+}+C_{6-14}$) for drainage areas I, IV and VII (see Fig. 13 for locations). GOR and dryness/lightness are only displayed from the first event exceeding 1 % of the maximum incremental oil or gas volume expelled in order to avoid plotting artefacts.

Modelled quality of the expelled oil, expressed by the ratio of $C_{6-14}/(C_{6-14}+C_{15+})$ (oil lightness), changes significantly over time (Fig. 15). In general, an increase in the oil lightness ratio can be observed through time with increasing maturation of the source rocks. Oil lightness reaches values up to 0.8 in drainage polygons I to IV, whereas values remain below 0.4 in the southern half of the study area, which has reached lower levels of kerogen transformation.

The most gas-prone area is drainage polygon I with 2969 x 10^9 Sm^3 gas expelled (Table 3, Fig. 16b). Drainage polygon I has up to now proven to be gas-prone (Table 3) with the large Frigg gas field and its satellites with a total of over 200 x 10^9 Sm^3 gas in-place. The drainage polygon containing the largest gas fields in the area, polygon VII, which includes the Sleipner fields, shows insufficient gas volume expelled to fill the observed structures. This is due to a modelling artefact related to the crudeness of the Middle Jurassic model, specifically the quality of Middle Jurassic depth and source rock maps. Large uncertainties are associated with the Base Middle Jurassic depth map since it was created by grid interpolation from Base Upper and Lower Jurassic maps and well tie operations.

Gas expulsion from the Heather Formation dominates in the area with 38 % of all gas expelled, while the Sleipner and Hugin Formations of Middle Jurassic age supply 26 %. The lower Draupne Formation also contributes significantly with 31 %, while the lower mature and highly oil-prone upper Draupne Formation only contributes 5 %. The Quaternary phase is certainly equally important for gas expulsion as it was for oil expulsion with 13 % of all gas expelled in model events 35 and 36. Gas dryness (C_1/C_1+C_{2-5}) tends to increase through time with increasing maturity of the source rocks to reach values between 0.28 and 0.37 in the Quaternary. Polygons I to IV show slightly higher values on average, while the southern half of the study area shows lower dryness ratios through time (Fig. 15i).

Modelled expelled gas-oil ratios (GOR) show a significant difference between the southern half of the area (polygons V to VIII) and the northern half (polygons I to IV) (Fig. 15). A general decrease in GOR until the Lower Eocene can be observed in the north which is followed by a gentle increase, whereas GOR values in the southern half of the study area remain at fairly constant levels. GORs rise to values up to 360 Sm^3/Sm^3 in the Quaternary in drainage polygon I (Fig. 15c), while GOR values remain below 200 Sm^3/Sm^3 in the southern part of the study area.
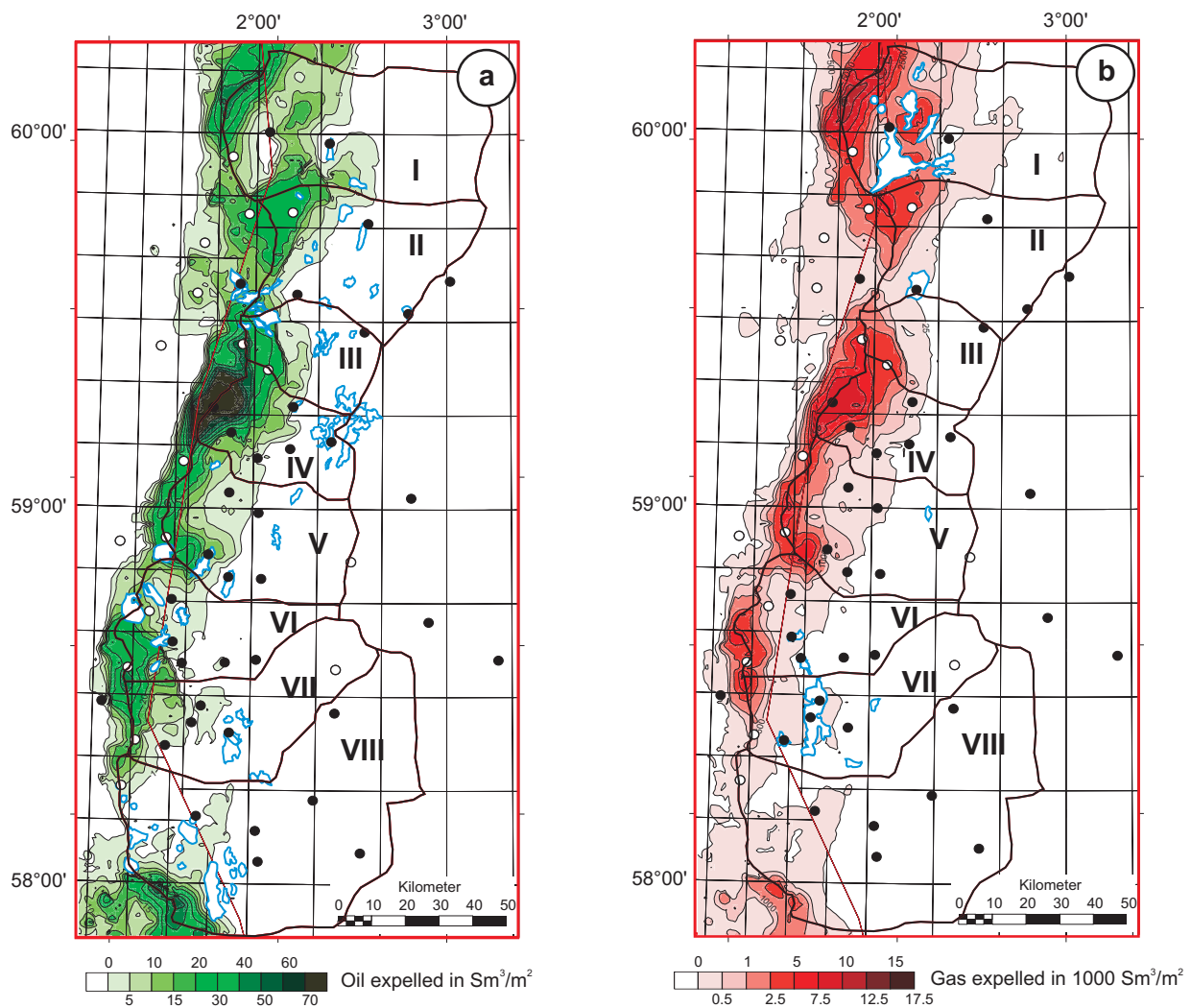
Fig. 16. Cumulative oil (a) and gas (b) volume in Sm^3/m^2 expelled from Upper and Middle Jurassic source rocks in the area. Drainage polygons are displayed in black lines. Locations of modelled wells are indicated by full circles, empty circles indicate pseudo-well locations. Blue outlines represent major oil fields in figure (a) and major gas fields in figure (b). Most oil-prone area with 16975 x10^6 Sm^3 expelled is drainage polygon IV, while the most gas-prone area with 2969 x10^9 Sm^3 of gas expelled is drainage polygon I.

Table 3
Expelled hydrocarbon volumes for all source events in all identified drainage polygons and calculated
generation accumulation efficiencies (GAE) for the respective polygons

Source Rock	HC Type	Drainage Polygon							
		I	II	III	IV	V	VI	VII	VIII
Upper Draupne	Heavy Oil (10^6 Sm^3)	3315	1074	874	2107	2290	1448	375	1093
	Light Oil (10^6 Sm^3)	1692	541	330	795	770	450	114	477
	Wet gas (10^9 Sm^3)	160	34	12	28	29	15	8	17
	Dry Gas (10^9 Sm^3)	55	12	4	9	10	6	4	9
Lower Draupne	Heavy Oil (10^6 Sm^3)	3480	1680	1677	6843	2998	2624	2048	3618
	Light Oil (10^6 Sm^3)	2526	1181	1181	4806	1703	1281	769	1717
	Wet gas (10^9 Sm^3)	449	179	167	577	285	94	25	58
	Dry Gas (10^9 Sm^3)	181	70	62	219	96	29	8	24
Heather	Heavy Oil (10^6 Sm^3)	2017	1627	1040	1093	651	1100	745	259
	Light Oil (10^6 Sm^3)	2184	1129	784	1331	638	872	345	144
	Wet gas (10^9 Sm^3)	832	94	91	420	321	209	54	94
	Dry Gas (10^9 Sm^3)	406	40	39	218	135	86	21	42
Middle Jurassic (Hugin & Sleipner Fm)	Heavy Oil (10^6 Sm^3)	0	0	0	0	0	8	18	1
	Light Oil (10^6 Sm^3)	0	0	0	0	0	224	109	2
	Wet gas (10^9 Sm^3)	530	156	79	180	150	177	56	6
	Dry Gas (10^9 Sm^3)	356	100	49	127	87	98	27	3
Total	Oil (10^6 Sm^3)	15214	7232	5886	16975	9050	8007	4523	7311
	Gas (10^9 Sm^3)	2969	685	503	1778	1113	714	203	253
In-place[a]	Oil (10^6 Sm^3)	4	60.9	140.3	459.5	142.8	183	108	215.6
	Gas (10^9 Sm^3)	210.9	71.3	20.7	4	130.8	98.9	274.8	71.3
GAE	Oil (%)	0.03	0.8	2.4	2.7	1.6	2.3	2.4	2.9
	Gas (%)	7.1	10.4	4.1	0.2	11.8	13.9	---	28.8

[a] In-place volumes are calculated from recoverable resources assuming average recovery factors of 40% for oil
and 80% for gas.

4.4. Implications for future exploration in the area and generation-accumulation efficiencies

Evaluation of the remaining hydrocarbon potential of the South Viking Graben is achieved by calculation of the generation-accumulation efficiency (GAE) for the respective drainage polygons in the study area. The GAE is defined as the fraction of the hydrocarbons discovered in-place of the total generated hydrocarbons in a specific area (Magoon and Valin, 1994). This fraction depends on the retention of oil and gas during primary and secondary migration, loss due to early charge before trap formation, as well as inadequate trap volume and seal capacity (Magoon and Valin, 1994; Lewan et al., 2002). In addition, volume will be lost in non-commercial micro-accumulations.

Since in-place volumes for fields and discoveries are commonly not reported, they must be calculated from reported estimates of recoverable reserves by application of average recovery factors. Volume estimates for UK fields (Eriksen et al., 2003) in the drainage polygons of this study have been combined with the estimates from NPD (2005). The published recovery factor values for oil fields vary greatly from only 25 % (Magoon and Valin, 1994) and 30 % (Barnard and Bastow, 1991) to 46 % as the average for the Norwegian Continental Shelf (NPD, 2005). Gas recovery is higher and is reported to reach values of 70 % (Kubala et al., 2003) and 80 % (Barnard and Bastow 1991). To calculate GAE values for the individual drainage polygons, recovery factors of 40 % for oil and 80 % for gas have been assumed. Calculated GAE values for the individual polygons for oil range from 0.03 %
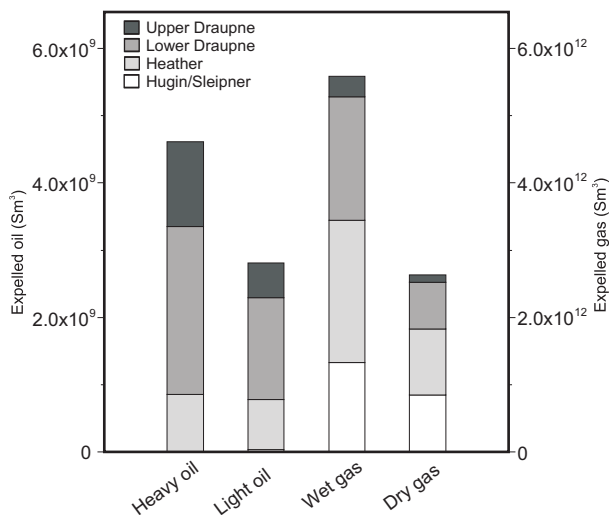

Fig. 17. Total expelled volume for all modelled pseudo-components for all source rock units. Most oil-prone source is the lower Draupne Formation with over 54 % of all oil expelled from this unit, while the most gas-prone unit is the Heather Formation with more than 37 % of all gas expelled.

(polygon I) to 2.9 % (polygon VIII) (Table 3), while GAEs for gas are somewhat higher ranging from 0.2 % (IV) to 28.8 % (VII) (Table 3). Modelled gas volumes in polygon VII are smaller than the observed volume. As discussed previously, this is most likely due to a modelling artefact related to the poor quality of the Top Middle Jurassic depth map. Given the large variation in published recovery factors, a high, middle and low case was chosen to calculate the in-place volumes for the evaluation of the GAE for the entire area (Table 4). Calculated GAE values for the entire area based on these numbers and modelling results as in Table 3 are shown in Table 4. The GAE for oil in the area ranges from 1.01 to 1.06 %, while the values for gas are between 9.67 and 12.89 %.

Table 4
Total generation-accumulation efficiencies (GAE) for the South Viking Graben

	Oil and Condensate (10^6 Sm³)			Gas (10^9 Sm³)		
Recoverable Volume[a]	391.2			463.28		
Recovery Factors	0.3	0.35	0.40	0.70	0.75	0.80
In-place Volume[a]	788	769	755	1059	908	795
Modelled Volume	74198			8218		
GAE %	**1.06**	**1.03**	**1.01**	**12.89**	**11.05**	**9.67**

[a] Commonly only recoverable volumes are reported by operators. Therefore in-place volumes have to be estimated using recovery factors for oil and gas fields. In-place volumes include Norwegian and UK fields within drainage polygons outlined in this study. NGL has been excluded (only 3.5% of total recoverable volume).

These values are not meaningful without a discussion and comparison to other petroleum systems. The mega petroleum systems of the South Viking Graben (including the UK resources) contain a total of 1.2 x 10^9 Sm³ oil equivalents and can be classified as significant in size according to Magoon and Schmoker (2000). By applying strictly the classification of Magoon and Valin (1994), the petroleum systems can be regarded as moderately efficient (GAE between 1% and 10%) for oil. Due to the extremely low values, the systems could almost be considered inefficient for oil. Considering the fact that Middle Jurassic gas volumes were probably underestimated, especially in drainage polygon VII, the systems can be regarded as moderately efficient for gas. Magoon and Valin (1994) discuss a number of petroleum systems with GAEs reaching values up to 36 %, while Dahl and Yükler (1991) report 13 % for oil and 30 % for gas in the Oseberg area of the Northern Viking Graben. Goff (1983) reports values between 19 and 25 % for oil in the Central and Eastern Shetland Basin. Compared to these values, the GAE values for the South Viking Graben are relatively low.

In order to judge the future potential of the area, we have also to take into account the individual processes and elements of the petroleum systems. Source rock analysis (Isaksen and Ledje, 2001; Justwan et al., 2005; Justwan et al., 2006) has shown that rich, high quality source rocks of considerable thickness are present in the area, which have expelled significant amounts of oil and gas (this study). The high generated volumes in combination with the overall low generation-accumulation efficiencies indicate therefore remaining potential in the area. Especially polygons I, II and V, showing the lowest GAEs for oil, have good potential for further exploration. These results should encourage further exploration in the area, especially before critical infrastructure is removed.

4.5. Case study – The petroleum systems of the Greater Balder Area

Key elements such as the characterisation of source rocks (Justwan et al., 2005), reservoired hydrocarbons (Justwan et al., 2006) and quantification of hydrocarbon generation allow the analysis of the petroleum systems of the study area. The Greater Balder area has been chosen as a case study for the analysis of the petroleum systems in the area and to test the rigidity of the modelling results.

The Greater Balder Area is located on the Utsira High in Blocks 25/10, 11 and 8 (Figs. 1, 18) and comprises the Balder, Ringhorne and Grane fields and the 25/8-4, 25/8-14S and 25/11-16 discoveries with a total of 184 x 10^6 Sm³ oil and 1.6 x 10^9 Sm³ gas recoverable (NPD, 2005). The main reservoir horizons are the Heimdal, Hermod and Balder Formation sandstones of Paleocene to Early Eocene age (Jenssen et al., 1993; Bergslien, 2002). The sands have excellent reservoir qualities with porosities of 31 to 36 % and permeabilities of 2 to 10 D in the Balder Field (Bergslien, 2002). The complex reservoir architecture and structural/stratigraphic trap result from depositional geometry of the reservoir body, differential compaction as well as deformation and sand remobilisation processes (Goff, 1983; Hanslien, 1987; Jenssen et al., 1993; Bergslien, 2002). The Eocene shales are the top seal for Tertiary
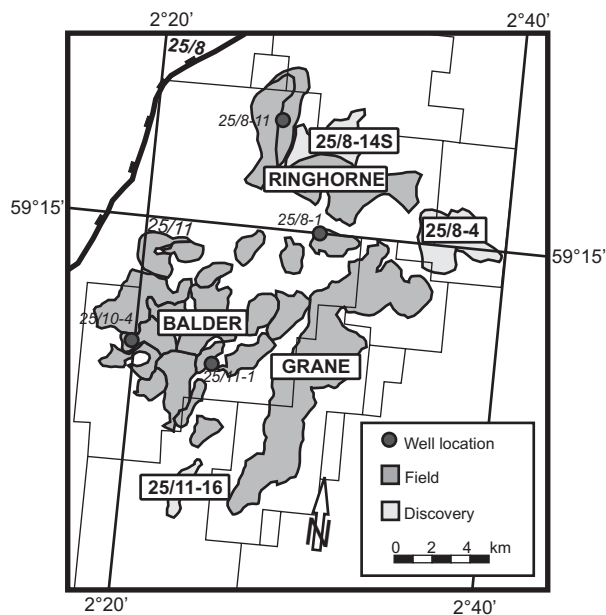
Fig. 18. Detail map of the Greater Balder Area (for overview map see Fig. 1). While the main reservoir units are of Paleocene age, an early Jurassic reservoir was encountered in Wells 25/8-11 and 25/10-4.

reservoirs (Jenssen et al., 1993), and trap formation in the South Viking Graben occurred in the early to late Eocene (Pegrum and Ljones, 1984; Jenssen et al., 1993). Hydrocarbons are also encountered in the Statfjord Formation sandstones of Lower Jurassic age in Well 25/10-4 (Balder) and 25/8-11 (Ringhorne). The Chalks of the Ekofisk Formation and the Paleocene shales form the caprock for the Lower Jurassic reservoirs. Trap formation occurred only slightly earlier for the Jurassic reservoirs than for the Tertiary reservoirs (D. Bergslien, pers. comm.). The hydrocarbons in this area are sourced exclusively from the Upper Jurassic Draupne Formation (Justwan et al., 2006). The Tertiary reservoirs appear to be charged with oil in two phases. The earlier charge phase was heavily biodegraded, while the later phase was only lightly degraded (Barnard and Bastow, 1991; Justwan et al., 2006). The hydrocarbons in the Jurassic reservoir of Ringhorne on the other hand show no sign of biodegradation (Justwan et al., 2006). The oil in the

Jurassic reservoirs in Balder appears to be non-biodegraded. It shows, however, minor amounts of 25-norhopane, an indication of a remnant phase of degradation (M. Richardson, pers. comm.).

The area is, as discussed earlier, the most oil-prone area in the South Viking Graben due to the thickness and quality of the Upper Jurassic source rocks in the kitchen area (polygon IV in Fig. 16). Generation and expulsion from the lower Draupne Formation dominates over generation from the upper Draupne Formation, and contribution from the Heather Formation and the Middle Jurassic is negligible (Table 3).

The main phase of expulsion from the Draupne Formation commenced in the Paleocene (61 Ma) and peaked during the Lower Miocene (23-15 Ma) (Figs 15d, e). Reduced subsidence and basin shallowing in the Middle and Upper Miocene led to lower expulsion, while the following Quaternary subsidence caused a short pulse of renewed generation and expulsion supplying over 9 % of the total oil yield in the area. Total expelled oil volume from the Heather Formation accounts for only 14 % of the total volume expelled from all source rocks in the kitchen area. Nearly 61 % of the Heather volume generated was lost because expulsion occurred before trap formation in the Eocene (34.5 Ma) (Fig. 15). The influence of Heather sourced hydrocarbons is therefore expected to be very small. These predictions agree with observed data in Justwan et al. (2006) showing a strong Draupne Formation signature for all hydrocarbons in this area.

Based on the results of the thermal maturity modelling, the main initial oil charge to the Tertiary reservoirs occurs contemporaneous with reservoir rock deposition. Less than 33 % of the oil total volume is estimated to be lost before trap formation. Temperature history reconstruction for the reservoir rocks from 1D sites in the area has shown that the Tertiary reservoirs never reached 70°C (Fig. 19). This value has been proposed as the regional maximum temperature for biodegradation (Justwan et al., 2006). Hydrocarbons in these reservoirs could therefore have been degraded since they first arrived in the reservoir. The second, later charge occurred in the Quaternary and diluted the heavy degraded oils. This mixture was subsequently only lightly degraded (Fig. 19). This is in good agreement with the observed situation in the Balder area where oils deriving from multiple charge phases have been described (Justwan et al., 2006). The Jurassic reservoired oil at Ringhorne is, however, not biodegraded, while the Jurassic reservoired oil at Balder shows only remnants of an earlier phase of biodegradation but no present biodegradation. The Jurassic reservoirs at Ringhorne have reached higher temperatures (68°C), very close to the cut-off temperature already in the Miocene (Fig. 19) and could have been pasteurised, effectively stopping biodegradation. Deep burial sterilisation or pasteurisation of reservoirs has been proposed as a mechanism by Wilhelms at al. (2001). The oils in the Jurassic
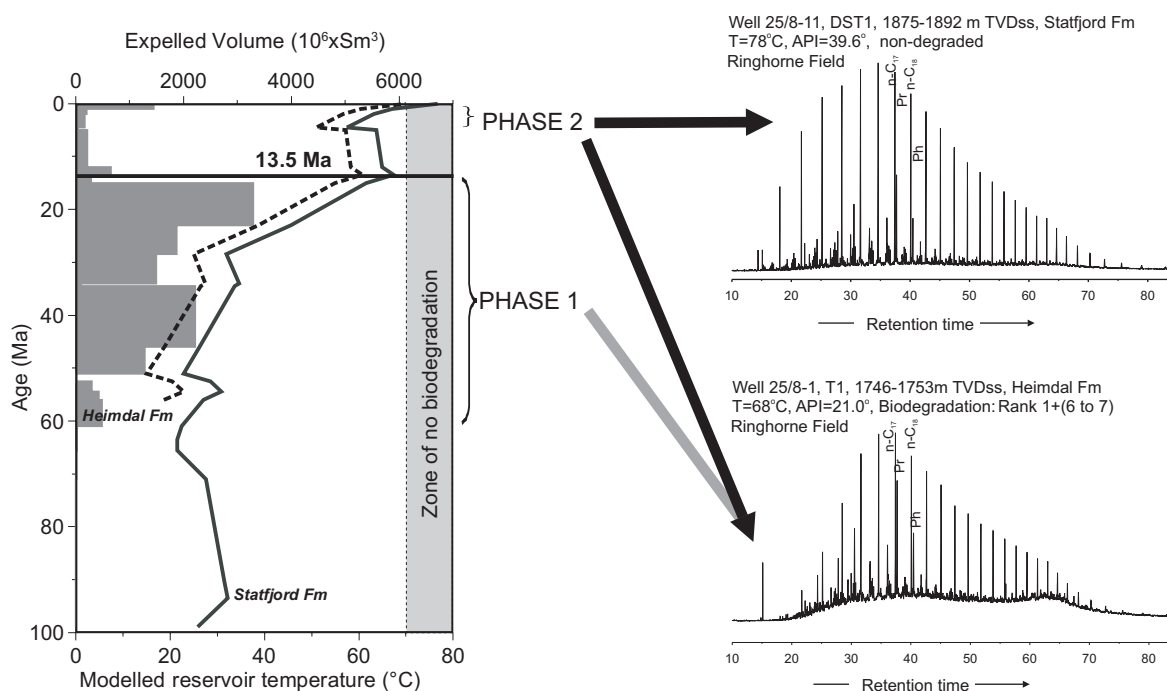
Fig. 19. A time-reservoir temperature plot displayed alongside the expelled Draupne Formation oil volumes (increments for events) offers a possible explanation for the occurrence of biodegraded and non-biodegraded oils in the Balder-Ringhorne area. The Heimdal reservoir, currently at its maximum temperature of 68°C, has been charged in two phases and was exposed to biodegradation since the beginning of the oil charge. The deeper Statfjord reservoir reached temperatures very close to 70°C, which is the cut-off temperature for biodegradation in the area (Justwan et al., 2006), already in the Miocene and could have been pasteurised. A later charge during phase 2 would therefore not be biodegraded. Another possible explanation for the non-degraded nature of the oil in the Jurassic reservoir is very late Quaternary charge when reservoir temperatures approached present day values of 78°C.

reservoirs could therefore be the result of charge after 13.5 Ma and could have reached the reservoir possibly after pasteurisation. Alternatively, if temperatures were not high enough for pasteurisation, the oils could be result of very late charge during the Quaternary, when reservoir temperatures approach the present day temperature of 78°C.

The origin of the Jurassic reservoired oils from this late charge phase is also supported by the thermal maturity of the Jurassic reservoired oils. It may seem as if all the oils in the area derived from the beginning of the main generation phase based on C_{29} sterane and C_{32} hopane isomerisation, as shown in Justwan et al. (2006). A closer look at the data, specifically the ratio of diasteranes to regular steranes, shows that the Jurassic samples from Ringhorne have a higher thermal maturity than oils in Tertiary reservoirs. Similar observations can be made for the oils in the Jurassic reservoirs in Balder (M. Richardson, pers. comm.). They are therefore likely to have derived from the second phase of oil expulsion when the Draupne Formation has reached a higher level of thermal maturity.

Total modelled GOR for drainage polygon IV of 105 Sm^3/Sm^3 matches well the observed value of 83 Sm^3/Sm^3 for the Balder and Ringhorne area. The discrepancy between modelled values and the low GOR in Grane of 19 Sm^3/Sm^3 is due to the fact the Grane oils have undergone significant biodegradation. Modelled GOR values for expelled hydrocarbons from the Upper Jurassic source rocks in the Greater Balder source kitchen are slightly increasing from values below 100 in the Eocene to reach 218 Sm^3/Sm^3 in the Quaternary (Fig. 15f). The slight increase in GOR can, however, not explain the presence of the gas cap in Balder alone. An alternative explanation for gas cap formation in the Balder Field is the effect of biodegradation which changes the oil composition and leads to strong increase in saturation pressure and possibly the development of a free gas phase (Larter and di Primio, 2005).

The petroleum system of the Greater Balder Area has been proven by source-oil correlation in Justwan et al. (2006) and can be named after the main source rock, the Draupne Formation, and the main reservoir rock, the Heimdal Formation, the Draupne-Heimdal (!) petroleum system. Figure 20 summarises the most important events for the Draupne-Heimdal (!) petroleum system in the South Viking Graben.

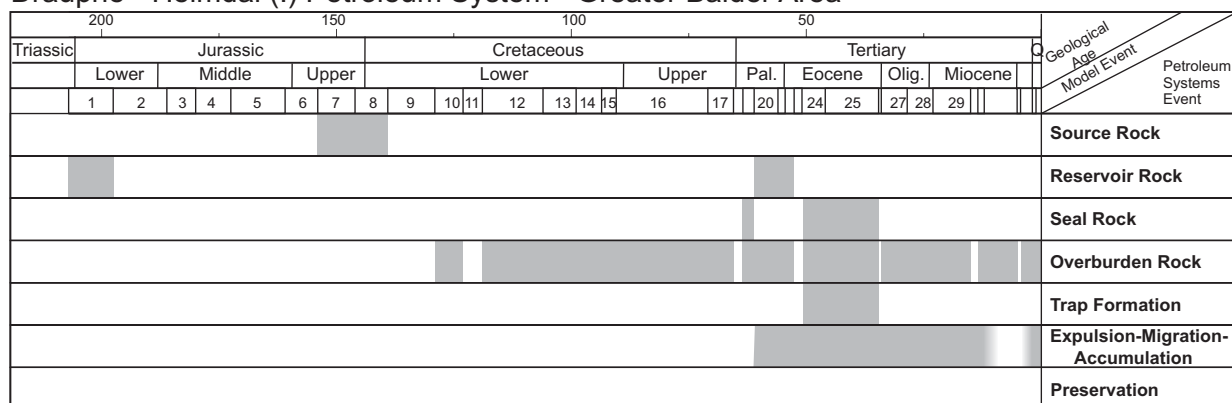## Draupne - Heimdal (!) Petroleum System - Greater Balder Area

Fig. 20. Petroleum systems chart for the Draupne-Heimdal (!) system in the Greater Balder Area. Hydrocarbon generation and expulsion occurs nearly exclusively from the Upper Jurassic Draupne Formation. Since the petroleum system remains active, there is no preservation time.

5. Conclusions

A detailed conceptual 1D basin model consisting of 36 isochronous geological events has been developed based on thorough analysis of stratigraphy and basin development of the South Viking Graben. Modelling results for 46 1D sites and 13 subsurface maps were subsequently employed to create a map-based pseudo-3D model in order to evaluate the timing and magnitude of hydrocarbon generation and expulsion and the remaining hydrocarbon potential in the area.

The validity of model was tested throughout including check parameters for individual 1D sites, validation of kinetics by comparison of modelled transformation ratios with ratios from Rock-Eval data and calibration of expulsion thresholds.

Two major phases of hydrocarbon expulsion can be observed in the area. The main phase for Upper Jurassic source rocks started in the Paleocene, peaked in the Lower Miocene and ended in the Middle Miocene. This period was followed by reduced expulsion as a result of basin shallowing. Due to different expulsion behaviour and kinetics, oil expulsion for Middle Jurassic source rocks started in the Lower Miocene, while gas generation began in the Eocene (51 Ma). A phase of renewed expulsion occured for all source rocks in the Quaternary as result of high subsidence rates during this period. This second phase of hydrocarbon generation and expulsion is responsible for 11 % of all oil and 13 % of all gas expelled. This event has increasing importance towards the south where higher Quaternary thicknesses are observed. The Middle Jurassic source rocks have at present reached levels of 70 % kerogen transformation in the deepest parts of the basin, whereas the Upper Jurassic Heather and lower Draupne Formation have nearly realised their entire hydrocarbon generation potential in the main parts of the graben. The modelling predicts that the shallower and highly oil-prone upper Draupne Formation has not reached transformation ratio values above 60 % in most of the graben area.

In total, 74198 x 10^6 Sm^3 of oil and 8218 x 10^9 Sm^3 gas have been expelled from Upper and Middle Jurassic sources. The lower Draupne Formation dominates the oil expulsion with over 54 % of all oil expelled, whereas the most gas-prone unit is the Heather Formation with more than 38 % of all gas expelled. Drainage polygon IV, which feeds the biggest cluster of oil accumulations in the area, the Balder, Ringhorne and Grane fields, has the most oil-prone kitchen area. The most gas-prone area is drainage polygon I, which feeds the cluster of gas fields in the Frigg area in the northern part of the study area.

The modelling results were used to investigate the petroleum systems of the Greater Balder Area. Hydrocarbon charge in the Greater Balder Area began contemporaneously with reservoir rock deposition, slightly before trap development in the Eocene. Hydrocarbons were received in two main charge phases almost exclusively from the Draupne Formation. The main phase of charge was severely degraded but subsequently diluted with fresh oil during

the second phase of Quaternary age. Secondary alteration and expelled gas-oil ratios in the Greater Balder Area suggest exsolution of gas from oil due to biodegradation as an alternative method for gas cap formation in the area. Comparison of modelled expelled hydrocarbon volumes in the South Viking Graben with volumes in-place allowed the calculation of generation accumulation efficiencies and evaluation of the remaining hydrocarbon potential of the area. Low generation-accumulation efficiencies for the area, approximately 1% for oil and 10% for gas, together with the presence of abundant high quality source rock suggest remaining hydrocarbon potential in the area. The low efficiencies should therefore encourage further exploration in this mature area of the North Sea, especially before removal of critical existing infrastructure.

Acknowledgements

References

Baird, R.A., 1986. Maturation and source rock evaluation of Kimmeridge Clay, Norwegian North Sea. AAPG Bulletin 70 (1), 1-11.

Barnard, P.C., Bastow, M.A., 1991. Petroleum generation, migration, alteration, entrapment and mixing in the central and northern North Sea. In: England, W.A., Fleet, A.J. (Eds.), Petroleum Migration. Geological Society Special Publication 59, pp. 167-190.

Behar, F., Vandenbroucke, M., Tang, Y., Marquis, F., Espitalié, J., 1997. Thermal cracking of kerogen in open and closed systems; determination of kinetic parameters and stoichiometric coefficients for oil and gas generation. Organic Geochemistry 26 (5-6), 321-339.

Berggren, W.A., Kent, D.V., Swisher, C.C., III, Aubry, M.P., 1995. A revised Cenozoic geochronology and chronostratigraphy. In: Berggren, W.A., Dennis, V.K., Aubry, M.-P., Hardenbol, J. (Eds.), Geochronology, Time Scales and Global Stratigraphic Correlation. SEPM Special Publication 54, pp. 129-212.

Bergslien, D., 2002. Balder and Jotun; two sides of the same coin? A comparison of two Tertiary oil fields in the Norwegian North Sea. Petroleum Geoscience 8 (4), 349-363.

Braun, R.L., Burnham, A.K., 1992. PMOD; a flexible model of oil and gas generation, cracking, and expulsion. Organic Geochemistry 19 (1-3), 161-172.

Brigaud, F., Vasseur, G., Caillet, G., 1992. Thermal state in the North Viking Graben (North Sea) determined from oil exploration well data. Geophysics 57 (1), 69-88.

Buchardt, B., 1978. Oxygen isotope palaeotemperatures from the Tertiary period in the North Sea area. Nature 275 (5676), 121-123.

Burley, S.D., 1993. Models of burial diagenesis for deep exploration plays in Jurassic fault traps of the central and northern North Sea. In: Parker, J.R. (Ed.), Petroleum Geology of Northwest Europe; Proceedings of the 4th Conference. Geological Society, London, pp. 1353-1375.

Burnham, A.K., 1989. A simple kinetic model of petroleum formation and cracking. Report UCID-21665, Lawrence Livermore National Laboratory.

Burnham, A.K., Dahl, B., 1993. Compositional Modelling of Kerogen Maturation. In: Øygard, K. (Ed.), Poster session from the 16th Meeting on Organic Geochemistry. Stavanger, pp. 241-246.

Burnham, A.K., Sweeney, J., 1989. Modeling the Maturation and Migration of Petroleum. Report UCRL-102602, Lawrence Livermore National Laboratory.

Cameron, T.D.J., Stoker, M.S., Long, D., 1987. The history of Quaternary sedimentation in the UK sector of the North Sea Basin. Journal of the Geological Society of London 144 (1), 43-58.

Cooles, G.P., Mackenzie, A.S., Quigley, T.M., 1986. Calculation of petroleum masses generated and expelled from source rocks. Organic Geochemistry 10 (1-3), 235-245.

Copestake, P., Sims, A., Crittenden, S., Hamar, G., Ineson, J., Rose, P., Tringham, M., Bathurst, P., 2003. Lower Cretaceous. In: Evans, D., Graham, C., Armour, A., Bathurst, P. (Eds.), The Millennium Atlas; Petroleum Geology of the Central and Northern North Sea. Geological Society, London, pp. 191-211.

Cornford, C., 1998. Source rocks and hydrocarbons of the North Sea. In: Glennie, K.W. (Ed.), Petroleum Geology of the North Sea; Basic Concepts and Recent Advances. Blackwell, Oxford, pp. 376-462.

Coward, M.P., Dewey, J., Hempton, M., Holroy, J., 2003. Tectonic evolution. In: Evans, D., Graham, C., Armour, A., Bathurst, P. (Eds.), The Millennium Atlas; Petroleum Geology of the Central and Northern North Sea. Geological Society, London, pp. 17-33.

Dahl, B., Augustson, J.H., 1993. The influence of Tertiary and Quaternary sedimentation and erosion on hydrocarbon generation in Norwegian offshore basins. In: Doré, A.G., Augustson, J.H., Hermanrud, C., Stewart, D.J., Sylta, Ø. (Eds.), Basin Modelling; Advances and Applications. NPF Special Publication 3, pp. 419-431.

Dahl, B., Meisingset, I., 1996. Prospect resource assessment using an integrated system of basin simulation and geological mapping software: examples from the North Sea. In: Doré, A.G., Sinding-Larsen, R. (Eds.), Quantification and Prediction of Petroleum Resources. NPF Special Publication 6, pp. 237-251.

Dahl, B., Yükler, A., 1991. The role of petroleum geochemistry in basin modeling of the Oseberg area, North Sea. In: Merrill, R.K.

(Ed.), Source and Migration Processes and Evaluation Techniques. AAPG Treatise of Petroleum Geology, pp. 65-85.

Eggen S., S., 1984. Modelling of subsidence, hydrocarbon generation, and heat transport in the Norwegian North Sea. In: Durand, B. (Ed.), Thermal Phenomena in Sedimentary Basins. Edition Techniprint, Paris, pp. 271-286.

Eriksen, S.H., Andersen, J.H., Grist, M., Stoker, S., Brzozowska, J., 2003. Oil and gas resources. In: Evans, D., Graham, C., Armour, A., Bathurst, P. (Eds.), The Millennium Atlas: Petroleum Geology of the Central and Northern North Sea. Geological Society, London, pp. 345-358.

Espitalié, J., Ungerer, P., Irwin, I., Marquis, F., 1988. Primary cracking of kerogens. Experimenting and modeling C_1, C_{2-5}, C_{6-15} and C_{15+} classes of hydrocarbons formed. Organic Geochemistry 13 (4-6), 893-899.

Færseth, R.B., 1996. Interaction of Permo-Triassic and Jurassic extensional fault-blocks during the development of the northern North Sea. Journal of the Geological Society of London 153 (6), 931-944.

Field, J.D., 1985. Organic geochemistry in exploration of the northern North Sea. In: Thomas, B.M., Doré, A.G., Larsen, R.M., Home, P.C., Eggen, S.S. (Eds.), Petroleum Geochemistry in Exploration of the Norwegian Shelf. Graham and Trotman, London, pp. 39-57.

Forbes, P.L., Ungerer, P., Kuhfuss, A.B., Riis, F., Eggen, S.S., 1991. Compositional modeling of petroleum generation and expulsion: trial application to a local mass balance in the Smørbukk Sør Field, Haltenbanken. AAPG Bulletin 75 (5), 873-893.

Fraser, S.I., Robinson, A.M., Johnson, H.D., Underhill, J.R., Kadolsky, D.G.A., Connell, R., Johannessen, E.P., Ravnas, R., 2003. Upper Jurassic. In: Evans, D., Graham, C., Armour, A., Bathurst, P. (Eds.), The Millennium Atlas: Petroleum Geology of the Central and Northern North Sea. Geological Society, London, pp. 157-189.

Ghazi, S.A., 1992. Cenozoic uplift in the Stord Basin area and its consequences for exploration. Norsk Geologisk Tidsskrift 72 (3), 285-290.

Goff, J.C., 1983. Hydrocarbon generation and migration from Jurassic source rocks in the E Shetland Basin and Viking Graben of the northern North Sea. Journal of the Geological Society of London 140 (3), 445-474.

Gradstein, F.M., Backstrom, S., 1996. Cainozoic biostratigraphy and palaeobathymetry, northern North Sea and Haltenbanken. Norsk Geologisk Tidsskrift 76 (1), 3-32.

Graue, E., Helland-Hansen, W., Johnson, J., Lomo, L., Nøttvedt, A., Ronning, K., Ryseth, A., Steel, R., 1987. Advance and retreat of Brent delta system, Norwegian North Sea. In: Brooks, J., Glennie, K.W. (Eds.), Petroleum Geology of Northwest Europe. Graham & Trotman, London, pp. 915-937.

Gregersen, U., Michelsen, O., Sørensen, J.C., 1997. Stratigraphy and facies distribution of the Utsira Formation and the Pliocene sequences in the northern North Sea. Marine and Petroleum Geology 14 (7-8), 893-914.

Hanslien, S., 1987. Balder. In: Spencer, A.M. (Ed.), Geology of the Norwegian Oil and Gas Fields. Graham & Trotman, Norwell, pp. 193-201.

Haq, B.U., Hardenbol, J., Vail, P.R., 1987. Chronology of fluctuating sea levels since the Triassic. Science 235 (4793), 1156-1167.

Hardenbol, J., Thierry, J., Farley, M.B., de Graciansky, P.C., Vail, P.R., 1998. Mesozoic and Cenozoic sequence chronostratigraphic framework of European basins. In: De Graciansky, P.C., Hardenbol, J., Jacquin, T., Vail, P.R. (Eds.), Mesozoic and Cenozoic Sequence Stratigraphy of European basins. SEPM Special Publication 60, pp. 3-13.

Hermanrud, C., Eggen, S., Larsen, R.M., 1991. Investigation of the thermal regime of the Horda Platform by basin modelling; implications for the hydrocarbon potential of the Stord Basin, northern North Sea. In: Spencer, A.M. (Ed.), Generation, accumulation, and production of Europe's hydrocarbons.

European Association of Petroleum Geoscientists Special Publication 1, pp. 65-73.

Husmo, T., Hamar, G.P., Høiland, O., Johannessen, E.P., Rømuld, A., Spencer, A.M., Titterton, R., 2003. Lower and Middle Jurassic. In: Evans, D., Graham, C., Armour, A., Bathurst, P. (Eds.), The Millennium Atlas: Petroleum Geology of the Central and Northern North Sea. Geological Society, London, pp. 129-155.

Isaksen, D., Tonstad, K., 1989. A revised Cretaceous and Tertiary lithostratigraphic nomenclature for the Norwegian North Sea. NPD Bulletin 5.

Isaksen, G.H., Ledje, K.H.I., 2001. Source rock quality and hydrocarbon migration pathways within the greater Utsira High area, Viking Graben, Norwegian North Sea. AAPG Bulletin 85 (5), 861-883.

Isaksen, G.H., Patience, R., van Graas, G., Jenssen, A.I., 2002. Hydrocarbon system analysis in a rift basin with mixed marine and nonmarine source rocks; the South Viking Graben, North Sea. AAPG Bulletin 86 (4), 557-591.

Jenkyns, H.G., Forster, A., Schouten, S., Sinninghe Damste, J., 2004. High temperatures in the Late Cretaceous Arctic Ocean. Nature 432, 888-892.

Jensen, R.P., Doré, A.G., 1993. A recent Norwegian Shelf heating event; fact or fantasy? In: Doré, A.G., Augustson, J.H., Hermanrud, C., Stewart, D.J., Sylta, Ø. (Eds.), Basin Modelling; Advances and Applications. NPF Special Publications 3, pp. 85-106.

Jenssen, A.I., Bergslien, D., Rye-Larsen, M., Lindholm, R.M., 1993. Origin of complex mound geometry of Paleocene submarine-fan sandstone reservoirs, Balder Field, Norway. In: Parker, J.R. (Ed.), Petroleum Geology of Northwest Europe; Proceedings of the 4th Conference. Geological Society, London, pp. 135-143.

Johnson, H.D., Fisher, M.J., 1998. North Sea plays; geological controls on hydrocarbon distribution. In: Glennie, K.W. (Ed.), Petroleum Geology of the North Sea; Basic Concepts and Recent Advances. Blackwell, Oxford, pp. 463-547.

Jones, E., Jones, B., Ebdon, C., Ewen, D., Milner, P., Plunkett, J., Hudson, G., Slater, P., Ross, J., Kubala, M., Jolley, D., Groves, S., Sawyers, M., Wathne, E., 2003. Eocene. In: Evans, D., Graham, C., Armour, A., Bathurst, P. (Eds.), The Millennium Atlas; Petroleum Geology of the Central and Northern North Sea. Geological Society, London, pp. 261-227.

Jordt, H., Faleide, J.I., Bjørlykke, K., Ibrahim, M.T., 1995. Cenozoic sequence stratigraphy of the central and northern North Sea Basin; tectonic development, sediment distribution and provenance areas. Marine and Petroleum Geology 12 (8), 845-879.

Justwan, H., Dahl, B., 2005. Quantitative hydrocarbon potential mapping and organofacies study in the Greater Balder Area, Norwegian North Sea. In: Doré, A.G., Vining, B. (Eds.), Petroleum Geology: North-West Europe and Global Perspectives - Proceedings of the 6th Petroleum Geology Conference. Geological Society, London, pp. 1317-1329.

Justwan, H., Dahl, B., Isaksen, G.H., 2006. Geochemical characterisation and genetic origin of oils and condensates in the South Viking Graben, Norway. Marine and Petroleum Geology 23 (2), 213-239.

Justwan, H., Dahl, B., Isaksen, G.H., Meisingset, I., 2005. Late to Middle Jurassic source facies and quality variations, South Viking Graben, North Sea. Journal of Petroleum Geology 28 (3), 241-268.

Keym, M., Dieckmann, V., Horsfield, B., Erdmann, M., Galimberti, R., Kua, L.-C., Leith, L., Podlaha, O., 2006. Source rock heterogeneity of the Upper Jurassic Draupne Formation, North Viking Graben and its relevance to petroleum generation studies. Organic Geochemistry 37 (2), 220-243.

Kubala, M., Bastow, M., Thompson, S., Scotchman, I., Øygard, K., 2003. Geothermal regime, petroleum generation and migration. In: Evans, D., Graham, C., Armour, A., Bathurst, P. (Eds.), The Millennium Atlas: Petroleum Geology of the Central and Northern North Sea. Geological Society, London, pp. 289-315.

Kyrkjebø, R., 1999. The Cretaceous-Tertiary of the northern North Sea: thermal and tectonic influences in a post-rift setting. PhD thesis, University of Bergen, Norway.

Larsen, R., M., Jaarvik, L.J., 1981. The geology of the Sleipner field complex. Norwegian Symposium on Exploration. Elsevier, Amsterdam, pp. NSE/15.

Larter, S.R., di Primio, R., 2005. Effects of biodegradation on oil and gas field PVT properties and the origin of oil rimmed gas accumulation. Organic Geochemistry 36 (2), 299-310.

Levitus, S., Boyer, T., 1994. World Ocean Atlas 1994 Volume 4: Temperature. Washington, U.S. Department of Commerce.

Lewan, M.D., Henry, M.E., Higley, D.K., Pitman, J.K., 2002. Material-balance assessment of the New Albany-Chesterian petroleum system of the Illinois basin. AAPG Bulletin 86 (5), 745-777.

Leythäuser, D., Schäfer, R.G., Yükler, A., 1982. Role of diffusion in primary migration of hydrocarbons. AAPG Bulletin 66, 408-429.

Løseth, H., Henriksen, S., 2005. A Middle to Late Miocene compression phase along the Norwegian passive margin. In: Doré, A.G., Vining, B. (Eds.), Petroleum Geology: North-West Europe and Global Perspectives - Proceedings of the 6th Petroleum Geology Conference. Geological Society, London, pp. 845-859.

Magoon, L.B., Schmoker, J.W., 2000. The total petroleum system. The natural fluid network that constrains the assessment unit, USGS.

Magoon, L.B., Valin, C.Z., 1994. Overview of petroleum system case studies. In: Magoon, L.B., Dow, W.G. (Eds.), The Petroleum System; From Source to Trap. AAPG Memoir 60, pp. 329-338.

Martinsen, O.J., Boen, F., Charnock, M.A., Mangerud, G., Nøttvedt, A., 1999. Cenozoic development of the Norwegian margin 60-64 degrees N; sequences and sedimentary response to variable basin physiography and tectonic setting. In: Fleet, A.J., Boldy, S.A.R. (Eds.), Petroleum Geology of Northwest Europe; Proceedings of the 5th Conference. Geological Society, London, pp. 293-304.

McKenzie, D., 1978. Some remarks on the development of sedimentary basins. Earth and Planetary Science Letters 40 (1), 25-32.

Miles, J.A., 1990. Secondary migration in the Brent sandstones of the Viking Graben and East Shetland Platform Basin: evidence from oil residues and subsurface pressure data. AAPG Bulletin 74 (11), 1718-1735.

Ministry of Petroleum and Energy 2005. Facts 2005 - The Norwegian Petroleum Activity. Norwegian Ministry of Petroleum and Energy, Oslo, 194 pp.

Mo, E.S., Throndsen, T., Andresen, P., Backstrom, S.A., Forsberg, A., Haug, S., Torudbakken, B., 1989. A dynamic deterministic model of hydrocarbon generation in the Midgard Field drainage area offshore Mid-Norway. Geologische Rundschau 78 (1), 305-317.

Mudge, D.C., Bujak, J.P., 1994. Eocene Stratigraphy of the North Sea Basin. Marine and Petroleum Geology 11 (2), 166-181.

Nadin, P.A., Kusznir, N.J., 1995. Palaeocene uplift and Eocene subsidence in the northern North Sea basin from 2D forward and reverse stratigraphic modelling. Journal of the Geological Society of London 152 (5), 833-848.

Neal, J.E., 1996. A summary of Paleogene sequence stratigraphy in Northwest Europe and the North Sea. In: Knox, R.W.O.B., Corfield, R.M., Dunay, R.E. (Eds.), Correlation of the Early Paleogene in Northwest Europe. Geological Society Special Publication 101, pp. 15-42.

NPD, 2005. The NPD's Fact-pages. (accessed 08.07.2005) http://www.npd.no/engelsk/cwi/pbl/en/index.htm.

Oakman, C.D., Partington, M.A., 1998. Cretaceous. In: Glennie, K.W. (Ed.), Petroleum Geology of the North Sea; Basic Concepts and Recent Advances. Blackwell, Oxford, pp. 294-349.

Odinsen, T., Reemst, P., van der Beek, P., Faleide, J.I., Gabrielsen, R.H., 2000. Permo-Triassic and Jurassic extension in the northern North Sea; results from tectonostratigraphic forward modelling. Dynamics of the Norwegian Margin. Geological Society Special Publication 167, pp. 830-103.

Østvedt, O.J., Blystad, P., Magnus, C., 2005. Assessment of undiscovered resources on the Norwegian Continental Shelf. In: Doré, A.G., Vining, B. (Eds.), Petroleum Geology: North-West Europe and Global Perspectives - Proceedings of the 6th Petroleum Geology Conference. Geological Society, London, pp. 55-64.

Partington, M.A., Mitchener, B.C., Milton, N.J., Fraser, A.J., 1993. Genetic sequence stratigraphy for the North Sea Late Jurassic and Early Cretaceous; distribution and prediction of Kimmeridgian-late Ryazanian reservoirs in the North Sea and adjacent areas. In: Parker, J.R. (Ed.), Petroleum Geology of Northwest Europe; Proceedings of the 4th Conference. Geological Society, London, pp. 347-370.

Pegrum, R.M., Ljones, T.E., 1984. 15/9 Gamma gas field offshore Norway, new trap type for North Sea Basin with regional structural implications. AAPG Bulletin 68 (7), 874-902.

Pepper, A.S., Corvi, P.J., 1995. Simple kinetic models of petroleum formation; Part III, Modelling an open system. Marine and Petroleum Geology 12 (4), 417-452.

Poulsen, N.E., Riding, J.B., 2003. The Jurassic dinoflagellate cyst zonation of subboreal northwest Europe. The Jurassic of Denmark and Greenland. Geological Survey of Denmark and Greenland Bulletin 1, pp. 115-144.

Rattey, R.P., Hayward, A.B., 1993. Sequence stratigraphy of a failed rift system; the Middle Jurassic to Early Cretaceous basin evolution of the central and northern North Sea. In: Parker, J.R. (Ed.), Petroleum Geology of Northwest Europe: Proceedings of the 4th Conference. Geological Society, London, pp. 215-249.

Rawson, P.F., Riley, L.A., 1982. Latest Jurassic-Early Cretaceous events and the "late Cimmerian unconformity" in North Sea area. AAPG Bulletin 66 (12), 2628-2648.

Riis, F., Fjeldskaar, W., 1992. On the magnitude of the late Tertiary and Quaternary erosion and its significance for the uplift of Scandinavia and the Barents Sea. In: Larsen R., M., Brekke, H., Larsen, B.T. (Eds.), Structural and Tectonic Modelling and its Application to Petroleum Geology. NPF Special Publication 1, pp. 163-185.

Ritter, U., Grøver, A., 2003. Adsorption of petroleum compounds in vitrinite: implications for petroleum expulsion from coal. International Journal of Coal Geology 62 (3), 183-191.

Rundberg, Y., Eidvin, T., 2005. Controls on the depositional history and architecture of the Oligocene-Miocene succession, northern North Sea. In: Wandås, B. (Ed.), Onshore-Offshore Relationships on the North Atlantic Margin. NPF Special Publication 12, pp. 207-238.

Sandvik, E.I., Young, W., Curry, D.J., 1992. Expulsion from hydrocarbon sources: the role of organic absorption. Organic Geochemistry 19 (1-3), 77-87.

Sejrup, H.P., Aarseth, I., Haflidason, H., Løvlie, R., Bratten, A., Tjostheim, G., Forsberg, C.F., Ellingsen, K.L., 1995. Quaternary of the Norwegian Channel; glaciation history and palaeoceanography. Norsk Geologisk Tidsskrift 75 (2-3), 65-87.

Steel, R., Ryseth, A., 1990. The Triassic-Early Jurassic succession in the northern North Sea; megasequence stratigraphy and intra-Triassic tectonics. In: Hardman, R.F.P., Brooks, J. (Eds.), Tectonic Events Responsible for Britain's Oil and Gas Reserves. Geological Society Special Publication 55, pp. 139-168.

Surlyk, F., Dons, T., Clausen, C.K., Higham, J., 2003. Upper Cretaceous. In: Evans, D., Graham, C., Armour, A., Bathurst, P. (Eds.), The Millennium Atlas; Petroleum Geology of the Central and Northern North Sea. Geological Society, London, pp. 213-233.

Sweeney, J., Burnham, A.K., 1990. Evaluation of a simple model of vitrinite reflectance based on chemical kinetics. AAPG Bulletin 74 (10), 1559-1570.

Thomas, B.M., Møller-Pedersen, P., Whitaker, M.F., Shaw, N.D., 1985. Organic facies and hydrocarbon distributions in the

Norwegian North Sea. In: Thomas, B.M., Doré, A.G., Larsen, R.M., Home, P.C., Eggen, S.S. (Eds.), Petroleum Geochemistry in Exploration of the Norwegian Shelf. Graham and Trotman, London, pp. 3-26.

Underhill, J.R., Partington, M.A., 1993. Jurassic thermal doming and deflation in the North Sea; implications of the sequence stratigraphic evidence. In: Parker, J.R. (Ed.), Petroleum Geology of Northwest Europe; Proceedings of the 4th Conference. Geological Society, London, pp. 337-345.

Ungerer, P., 1993. Modelling of petroleum generation and expulsion; an update to recent reviews. In: Doré, A.G., Augustson, J.H., Hermanrud, C., Stewart, D.J., Sylta, Ø. (Eds.), Basin Modelling; Advances and Applications. NPF Society Special Publication 3, pp. 219-232.

Ungerer, P., Burrus, J., Doligez, B., Chenet, P.Y., Bessis, F., 1990. Basin evaluation by integrated two-dimensional modeling of heat transfer, fluid flow, hydrocarbon generation, and migration. AAPG Bulletin 74 (3), 309-335.

Vollset, J., Doré, A.G., 1984. A revised Triassic and Jurassic Lithostratigraphic Nomenclature of the Norwegian North Sea. Norwegian Petroleum Directorate Bulletin 59.

Wei, Z.P., Hermanrud, C., Lerche, I., 1990. Numerical basin modelling of the Sleipner Field, North Sea. Terra Nova 2 (1), 31-42.

Wilhelms, A., Larter, S.R., Head, I., Farrimond, P., di Primio, R., Zwach, C., 2001. Biodegradation of oil in uplifted basins prevented by deep-burial sterilization. Nature 411 (6841), 1034-1037.

Zachos, J., Pagani, M., Sloan, L., Thomas, E., Billups, K., 2001. Trends, rhythms, and aberrations in global climate 65 Ma to present. Science 292, 686-693.

Ziegler, P.A., 1990. Tectonic and palaeogeographic development of the North Sea rift system. In: Blundell, D.J., Gibbs, A.D. (Eds.), Tectonic Evolution of the North Sea Rifts. Oxford University Press, New York, pp. 1-36.